

Optimal guidance and estimation of a 2D diffusion-advection process by a team of mobile sensors [★]

Sheng Cheng ^a, Derek A. Paley ^b

^a *University of Illinois Urbana-Champaign*

^b *University of Maryland, College Park*

Abstract

This paper describes an optimization framework to design guidance for a possibly heterogeneous team of multiple mobile sensors to estimate a spatiotemporal process modeled by a 2D diffusion-advection process. Owing to the abstract linear system representation of the process, we apply the Kalman-Bucy filter for estimation, where the sensors provide linear outputs. We propose an optimization problem that minimizes the sum of the trace of the covariance operator of the Kalman-Bucy filter and a generic mobility cost of the mobile sensors, subject to the sensors' motion modeled by linear dynamics. We establish the existence of a solution to this problem. Moreover, we prove convergence to the exact optimal solution of the approximate optimal solution. That is, when evaluating these two solutions using the original cost function, the difference becomes arbitrarily small as the approximation gets finer. To compute the approximate solution, we use Pontryagin's minimum principle after approximating the infinite-dimensional terms originating from the diffusion-advection process. The approximate solution is applied in simulation to analyze how a single mobile sensor's performance depends on two important parameters: sensor noise variance and mobility penalty. We also illustrate the application of the framework to multiple sensors, in particular the performance of a heterogeneous team of sensors.

Key words: Infinite-dimensional systems; Multi-agent systems; Modeling for control optimization; Guidance navigation and control.

1 Introduction

The modern manufacturing industry has benefited from the advantages of mobile robots for their reliability, economic efficiency, safety, and ease of use. However, the monitoring and control of large-scale spatiotemporal processes, e.g., oil spills, harmful algal blooms, and forest fires, have relied heavily on human operators. These events can pose health threats, cause severe environmental issues, and incur substantial financial costs. In such a situation, mobile robots can replace the human operators and carry out the tasks intelligently and cooperatively so long as they are informed about the environment and guided with proper methods.

Spatiotemporal processes evolve in both space and time and, hence, they can be treated as dynamical systems whose dynamics are modeled by partial differential equa-

tions (PDEs). It is generally impossible to completely identify the state of a PDE-modeled system, also known as a distributed parameter system (DPS), with a finite number of sensors. Hence, an observer for the DPS is necessary. For system-theoretical results on the observability of parabolic PDEs, refer to [24, 25]. Early designs of the observer include least-square filtering methods for systems governed by linear [28] and nonlinear [26] partial differential equations.

For a DPS whose infinite-dimensional dynamics is linear with additive Gaussian noise, an infinite-dimensional Kalman-Bucy filter (KF), which is an extension to its finite-dimensional analog [4, 22], can be applied. The infinite-dimensional version of the KF first appeared in [1]. The key to an infinite-dimensional KF is the evolution of the estimation error's covariance, which is operator-valued and can be solved via Riccati equations whose properties have been discussed in [6, 7]. For numerical approximation and computational issues, approximation results are summarized in [8] for the infinite-dimensional algebraic Riccati equations of a linear-quadratic regulator. However, often the distur-

[★] This paper was not presented at any IFAC meeting. Corresponding author Sheng Cheng Tel. +1 217 979 8496.

Email addresses: chengs@illinois.edu (Sheng Cheng), dpaley@umd.edu (Derek A. Paley).

bance to a system may not be Gaussian, in which case an H_2 - or H_∞ -observer design is favorable [31, 41].

We categorize the design of an observer for a PDE-modeled system by sensor location, i.e., on the boundary or in the interior of the PDE's domain. For sensors placed on the boundary, one may design observers based on boundary measurements. The challenge in using boundary measurements is that the output operator is unbounded when characterized in an abstract linear system. A tutorial paper [19] reviews the conditions for the well-posedness of the dual control problem with boundary inputs. One approach to boundary observer design is backstepping [23, 37], which stabilizes the observer using a Volterra transformation that transforms the original system to a stable target system and passes on the stability to the observer via its inverse transformation. Optimization techniques, e.g., a linear-quadratic estimator [32], have been proposed for boundary sensors using the method of variation.

For static in-domain sensors, a network can be deployed for estimating a PDE-modeled system. The problem is how to place the sensors to yield effective estimation, which is referred to as sensor placement. The solution is to select the sensor placement that yields optimal performance for certain criteria. The trace of the covariance operator of the KF, which quantifies the uncertainty of the estimate, is a common choice of the cost function to be minimized [2]. A similar problem is investigated in [45], which establishes the well-posedness of the sensor placement problem and its approximation with the cost function being the trace of the covariance operator. The same criterion has been applied to sensor placement of the Boussinesq equation [20]. In [34], a randomized observability constant is minimized by choosing suitable shapes and locations of the sensors. Note that observability may not be a useful criterion [45] based on the analysis of its dual, controllability. Specifically, maximizing the minimum eigenvalue of the controllability gramian is not useful (for actuator placement) [30], because the minimum eigenvalue approaches zero as the dimension of approximation increases in computation. Geometric approaches can also be applied to sensor placement, e.g., using the centroidal Voronoi tessellation [16] and combining the transfer-function model with geometric rules [40].

A variation of the sensor placement problem includes mobility of the sensors. In this scenario, a guidance policy is necessary to take advantage of the additional degree of freedom induced by mobility, which also makes the problem more complicated by introducing the dynamics of the mobile sensors. One may design sensor guidance using Lyapunov-based methods, where the guidance is constructed to make the derivative of the Lyapunov function negative. The Lyapunov function is usually designed to contain (quadratic) terms involving the PDE state and the sensor guidance [13, 18]. The

Lyapunov-based guidance can further be used in monitoring a hazardous environment where the regions of high information density reduce sensor longevity. Such guidance is combined with a switching policy to balance the conflicting needs of information collection and sensor life span [15].

Optimization can also be applied to design sensor guidance, where the guidance (or the trajectory) of the sensor is selected to minimize a cost function. An early work [9] proposes an optimization problem that minimizes the weighted sum of the guidance effort for steering a sensor and the mean-square estimation error at a terminal time. In [12], the sensors are guided to the location that yields the maximum value of the estimation kernel. In [21], receding horizon guidance is proposed to find the sensor path that maximizes mutual information between sensor measurements and the predicted state of the PDE.

This paper proposes an optimization framework that designs guidance for a team of mobile sensors to estimate a 2D diffusion-advection process using a centralized KF. The cost to be minimized is the sum of two terms: the trace of the covariance operator of the KF, called the *uncertainty cost*, which quantifies the uncertainty of the estimation error and the *mobility cost* associated with the sensors' motion. The covariance operator of the KF, which is the solution of an operator-valued Riccati equation, has been studied in [6]. Specifically, conditions for the existence of Bochner integrable solutions (with values in the Schatten p -class) of an operator-valued Riccati equation are established. The Bochner integrable solutions yield simple numerical quadratures for computation of the covariance operator, which is demonstrated in sensor placement [6] and sensor trajectory planning [7]. Both problems minimize the trace of a weighted covariance operator, whereas the latter has the sensors' dynamics as the constraint.

In our formulation, factors related to the mobile sensor platforms are integrated in addition to reducing the estimation uncertainty only [7]. Specifically, the integration is reflected by the mobility cost, which can be interpreted as the penalty associated with motion. Our formulation supports various types of cost functions for evaluating the cost or penalty induced from mobility. In prior work, the mobility cost is either limited to a quadratic guidance effort [9] or cast as a general function of the guidance without detailed discussion [2, 5]. Furthermore, the formulation permits treating the proposed problem as an optimal control problem, where we show both the uncertainty cost and the mobility cost are continuous mappings of the sensors' guidance. We use the techniques for the existence of an optimal control [43, Theorem 6.1.4] to establish the existence of a solution to our problem.

To compute an optimal solution, approximations of the infinite-dimensional terms are necessary. Our treatment

of the proposed problem (and its approximation) permits the application of a two-point boundary value problem derived using Pontryagin’s minimum principle. After restricting the admissible guidance functions to a stringent set (with a reasonable physical interpretation), we establish convergence to an exact optimal solution of an approximate optimal solution, i.e., the cost difference between the original and approximate solutions becomes arbitrarily small as the dimension of approximation increases. The convergence result justifies the use of the approximation and affirms that the performance of an approximate solution is arbitrarily close to the performance of an exact solution.

We implement the solution method numerically in simulations to evaluate and analyze the performance of a single sensor and multiple sensors. The flow field that yields advection is set to drift the sensor platforms under realistic conditions. It has been observed that the flow field is leveraged by the optimal guidance to reduce the mobility cost in both cases of a single sensor and a team of homogeneous sensors. Simulations with a team of heterogeneous sensors suggest that such a team can reduce the cost of investment with only a minor degradation in the overall performance.

The contributions of this paper are threefold. First, we propose a guidance policy for a team of mobile sensors to estimate a 2D diffusion-advection process by solving a newly formulated optimization problem that minimizes the trace of the covariance operator plus a generic cost of the sensors’ motion subject to sensor platform dynamics. The resulting guidance minimizes the estimation uncertainty while taking care of the sensor-oriented concerns. The formulation with a generic mobility cost applies to a wide range of applications, e.g., accumulated exposure to hazards, guidance effort, or distance to terminal rendezvous locations. The mobility cost is incorporated into the design process, unlike prior work that minimized the uncertainty cost only [7]. Second, we establish realistic conditions for the existence of a solution to the proposed problem. Third, we establish conditions for convergence to an exact optimal solution of the approximate optimal solution. When evaluating these two solutions using the original cost function, the difference gets arbitrarily small as the approximation gets finer.

The problem studied in this paper is an extension of the optimal guidance problem for a 1D diffusion process [10]. It is the dual problem of the one studied in [11], which simultaneously designs guidance and actuation of a team of mobile actuators to control a 2D diffusion-advection process.

The remainder of the paper is organized as follows. Section II introduces the dynamics of the sensors, an abstract linear-system representation of the diffusion-advection process, the measurement model, and the infinite-dimensional Kalman-Bucy filter. Section III

states the problem formulation and establishes conditions for the existence of a solution to the problem. Section IV proves the convergence to the exact optimal solution of the approximate optimal solution and introduces a solution method to obtain optimal guidance. Section V includes the simulation results of multiple parameter studies: a single sensor, a team of homogeneous sensors, and a team of heterogeneous sensors. Section VI summarizes the paper and discusses ongoing work.

2 Background

2.1 Notation and terminology

The paper adopts the following notation. The symbols \mathbb{R} and \mathbb{R}^+ denote the set of real numbers and the set of nonnegative real numbers, respectively. The n -ary Cartesian power of a set M is denoted by M^n . The notation $X_1 \hookrightarrow X_2$ means that the space X_1 is densely and continuously embedded in X_2 . The norm in a finite- and infinite-dimensional space is denoted by $|\cdot|$ and $\|\cdot\|$, respectively, with subscripts indicating its type. The space of all bounded linear operators from space X to space Y is denoted by $\mathcal{L}(X; Y)$ or $\mathcal{L}(X)$ if $Y = X$. We define the space of continuous mappings by $C(I; X) = \{F : I \rightarrow X \text{ such that } t \mapsto F(t) \text{ is continuous in } \|\cdot\|_X\}$ with the sup norm $\|F(\cdot)\|_{C(I; X)} = \sup_{t \in I} \|F(t)\|_X$. For a Hilbert space \mathcal{H} equipped with inner product $\langle \cdot, \cdot \rangle$ and $\phi_1, \phi_2 \in \mathcal{H}$, define $\phi_1 \circ \phi_2 \in \mathcal{L}(\mathcal{H})$ by $(\phi_1 \circ \phi_2)\psi = \phi_1 \langle \phi_2, \psi \rangle$ for all $\psi \in \mathcal{H}$. The superscript $*$ denotes an optimal variable, whereas * denotes the adjoint of a linear operator. The transpose of a matrix A is denoted by A^\top . An $n \times n$ -dimensional diagonal matrix with elements of vector $[a_1, a_2, \dots, a_n]$ on the main diagonal is denoted by $\text{diag}(a_1, a_2, \dots, a_n)$. The i th element of a vector v is $[v]_i$. We follow the terminology of [11]: guidance refers to steering the dynamics of the mobile sensor. For an optimization problem

$$\begin{aligned} & \underset{x}{\text{minimize}} && J(x) \\ & \text{subject to} && x \in C, \end{aligned} \tag{P0}$$

we use $J_{(P0)}(x)$ to denote the cost function of (P0) evaluated at x . Specifically, $J_{(P0)}^*(x^*)$ indicates that the optimal value of (P0) is attained when the cost function is evaluated at an optimal solution x^* .

2.2 Dynamics of the mobile sensors

Assume each of the m_s mobile sensors has the linear dynamics

$$\dot{\zeta}_i(t) = \alpha_i \zeta_i(t) + \beta_i p_i(t), \quad \zeta_i(0) = \zeta_{i,0}, \tag{1}$$

where $\zeta_i(t) \in \mathbb{R}^n$ and $p_i(t) \in P_i \subset \mathbb{R}^m$ are the state and the guidance of sensor i at time t , respectively. The state

ζ_i contains the 2D location of sensor i and hence $n \geq 2$. Assume that system (1) is controllable. One special case of (1) would be a single integrator, where $\zeta_i(t) \in \mathbb{R}^2$ is the location, $p_i(t) \in \mathbb{R}^2$ is the velocity command, and α_i and β_i are the zero matrix and identity matrix, respectively.

For conciseness, we concatenate the states and guidance of all m_s sensors, respectively, and use one dynamical equation to describe the dynamics of all agents:

$$\dot{\zeta}(t) = \alpha\zeta(t) + \beta p(t), \quad \zeta(0) = \zeta_0, \quad (2)$$

where matrices α and β are assembled from α_i and β_i for $i \in \{1, 2, \dots, m_s\}$, respectively, and are consistent with the concatenation for ζ and p . The controllability of the concatenated system (2) inherits that of each individual system (1). With a slight abuse of notation, we use n for the dimension of $\zeta(t)$ and m for the dimension of $p(t)$. Define the admissible set of guidance $P := P_1 \times P_2 \times \dots \times P_{m_s}$ such that $p(t) \in P$ for $t \in [0, t_f]$.

2.3 Abstract linear system

Consider the following inhomogeneous diffusion-advection equation over a smooth and bounded 2D spatial domain Ω :

$$\frac{\partial z(x, y, t)}{\partial t} = a\nabla^2 z(x, y, t) - \mathbf{v} \cdot \nabla z(x, y, t) + w(x, y, t) \quad (3)$$

$$z(x, y, 0) = \hat{z}(x, y, 0) + w_0(x, y) \quad (4)$$

$$z(x, y, t)|_{(x, y) \in \partial\Omega} = 0, \quad (5)$$

where $(x, y) \in \Omega$, $t \in [0, t_f]$, $a > 0$ is the diffusion coefficient, and $\mathbf{v} \in \mathbb{R}^2$ is the flow that yields advection. The initial condition $z(\cdot, \cdot, 0)$ is perturbed around its nominal value $\hat{z}(\cdot, \cdot, 0)$ by an additive zero-mean Gaussian noise $w_0(\cdot, \cdot)$. The dynamics (3) is subject to an additive zero-mean Gaussian noise $w(\cdot, \cdot, t)$ with variance $Q(t)$, which is nonnegative and self-adjoint. The state noise $w(\cdot, \cdot, t)$ and initial noise $w_0(\cdot, \cdot)$ are mutually independent for all t .

For simplicity, represent the PDE state in (3) by an abstract linear system whose state variable $\mathcal{Z}(t)$ represents $z(\cdot, \cdot, t)$ at time t , such that

$$\dot{\mathcal{Z}}(t) = \mathcal{A}\mathcal{Z}(t) + w(t), \quad \mathcal{Z}(0) = \hat{\mathcal{Z}}_0 + w_0, \quad (6)$$

where \mathcal{Z} belongs to a Hilbert space \mathcal{H} with inner product $\langle \cdot, \cdot \rangle$ and induced norm $\|\cdot\|_{\mathcal{H}}$. Here, the variable \mathcal{Z} is the state of the DPS and space $\mathcal{H} = L^2(\Omega)$ is the state space. The operator \mathcal{A} is defined as $\mathcal{A}\psi = a\nabla^2\psi - \mathbf{v} \cdot \nabla\psi$ with $\psi \in \text{Dom}(\mathcal{A}) = \{\psi \in H_0^1(\Omega), \nabla^2\psi \in L^2(\Omega)\} = H^2(\Omega) \cap H_0^1(\Omega)$ [14]. Let $\mathcal{S}(\cdot)$ be the strongly continuous semigroup generated by \mathcal{A} .

The measurement by sensor i depends on the sensor's location such that

$$y_i(t) = \mathcal{C}_i^*(M_0\zeta_i(t), t)\mathcal{Z}(t) + v_i(t), \quad (7)$$

where M_0 is a matrix with appropriate dimension such that $M_0\zeta_i(t) \in \mathbb{R}^2$ is the location of sensor i and $\mathcal{C}_i^*(M_0\zeta_i(t), t) \in \mathcal{L}(\mathcal{H}; \mathbb{R})$ is the output operator that has an integral kernel $\mathcal{C}_i(M_0\zeta_i(t), t) \in L^2(\Omega)$ such that

$$\mathcal{C}_i^*(M_0\zeta_i(t), t)\phi = \iint_{\Omega} \mathcal{C}_i(M_0\zeta_i(t), t)(x, y)\phi(x, y)dx dy$$

for $\phi \in \mathcal{H}$. Additive zero-mean Gaussian noise $v_i(t)$ with variance σ_i^2 is included in the measurement.

The measurement can have many types, e.g., pointwise [9, 24, 25], interval integral [7, 18], interval average [17], and Gaussian-type kernel [7]. Later in the simulation section, we will use a time-invariant kernel given by the square-shaped average

$$\begin{aligned} &\mathcal{C}_i(M_0\zeta_i(t))(x, y) \\ &= \begin{cases} \frac{1}{4r_i^2} & \text{if } [x] - M_0\zeta_i(t) \in [-r_i, r_i] \times [-r_i, r_i] \\ 0 & \text{otherwise,} \end{cases} \end{aligned} \quad (8)$$

where $2r_i$ is the length of the side of the square at time t .

The measurements $y(t) \in \mathbb{R}^{m_s}$ of all sensors are compactly written as

$$y(t) = \mathcal{C}^*(M\zeta(t), t)\mathcal{Z}(t) + v(t), \quad (9)$$

where $\mathcal{C}^*(M\zeta(t), t)$ is an operator-valued vector $\mathcal{C}^*(M\zeta(t), t) := [\mathcal{C}_1^*(M_0\zeta_1(t), t), \dots, \mathcal{C}_{m_s}^*(M_0\zeta_{m_s}(t), t)]^\top$ and $M \in \mathbb{R}^{2m_s \times n}$ is a matrix such that $M\zeta(t)$ is a vector of locations of the sensors, i.e., $(M\zeta(t))^\top = [(M_0\zeta_1(t))^\top, \dots, (M_0\zeta_{m_s}(t))^\top]$. We sometimes use $\mathcal{C}(t)$ for brevity instead of $\mathcal{C}(\zeta(t), t)$, because the sensor state $\zeta(t)$ is a function of t . The measurement noise $v(t)$ is a zero-mean Gaussian vector with covariance $R := \text{diag}(\sigma_1^2, \sigma_2^2, \dots, \sigma_{m_s}^2)$. Assume the noise $w_0(\cdot, \cdot)$, $w(\cdot, \cdot, t)$, and $v(t)$ are mutually independent for all t .

2.4 Kalman-Bucy filter

Analogous to a finite-dimensional linear system, the infinite-dimensional linear system (6) and (9) admits a Kalman-Bucy filter (KF). For the derivation of the KF of an abstract linear system, one may refer to [28, 33]. The estimation $\hat{\mathcal{Z}}(t)$ of the state $\mathcal{Z}(t)$ can be updated from the measurement $y(t)$ by

$$\dot{\hat{\mathcal{Z}}}(t) = \mathcal{A}\hat{\mathcal{Z}}(t) + \Pi(t)\mathcal{C}(t)R^{-1}(y(t) - \hat{y}(t)), \quad (10)$$

$$\hat{y}(t) = \mathcal{C}^*(t)\hat{\mathcal{Z}}(t), \quad (11)$$

with initial condition $\hat{\mathcal{Z}}(0) := \hat{\mathcal{Z}}_0$. The predicted observation of the estimated system is denoted by $\hat{y}(t)$. The covariance operator of the estimation error $\Pi(t) := \mathbb{E}[(\mathcal{Z}(t) - \hat{\mathcal{Z}}(t)) \circ (\mathcal{Z}(t) - \hat{\mathcal{Z}}(t))]$ satisfies the following operator Riccati equation:

$$\begin{aligned} \dot{\Pi}(t) = & \mathcal{A}\Pi(t) + \Pi(t)\mathcal{A}^* + Q(t) \\ & - \Pi(t)\bar{\mathcal{C}}\bar{\mathcal{C}}^*(t)\Pi(t), \end{aligned} \quad (12)$$

where $\bar{\mathcal{C}}\bar{\mathcal{C}}^*(t)$ is a compact representation of $\mathcal{C}(t)R^{-1}\mathcal{C}^*(t)$. The initial condition $\Pi(0)$ is given as the covariance operator Π_0 of the initial estimation error $\Pi_0 := \mathbb{E}[(\mathcal{Z}(0) - \hat{\mathcal{Z}}(0)) \circ (\mathcal{Z}(0) - \hat{\mathcal{Z}}(0))]$ [45], which is the variance of w_0 and is nonnegative and self-adjoint.

Definition 2.1 ([6, Definition 1.2]) *The trace operator $\text{Tr}(\cdot) : \mathcal{L}(\mathcal{H}) \rightarrow \mathbb{R}$ is defined as $\text{Tr}(\mathcal{G}) = \sum_{i=1}^{\infty} \langle \phi_i, \mathcal{G}\phi_i \rangle$ for nonnegative $\mathcal{G} \in \mathcal{L}(\mathcal{H})$, where $\{\phi_i\}_{i=1}^{\infty}$ is an arbitrary orthonormal basis that spans \mathcal{H} .*

Note that $\text{Tr}(\mathcal{G})$ is independent of the choice of the orthonormal basis.

Definition 2.2 ([7, Definition 3.2]) *Let \mathbb{H} be a separable complex Hilbert space. For $1 \leq q < \infty$, let $\mathcal{J}_q(\mathbb{H})$ denote the set of all bounded operators $\mathcal{L}(\mathbb{H})$ such that $\text{Tr}([A]^q) < \infty$, where $[A] := \sqrt{A^*A}$. If $A \in \mathcal{J}_q(\mathbb{H})$, then the \mathcal{J}_q -norm of A is defined as $\|A\|_{\mathcal{J}_q(\mathbb{H})} := (\text{Tr}([A]^q))^{1/q}$.*

The classes $\mathcal{J}_1(\mathcal{H})$ and $\mathcal{J}_2(\mathcal{H})$ are known as the space of trace-class operators and the space of Hilbert-Schmidt operators, respectively. Note that a continuous embedding $\mathcal{J}_{q_1}(\mathcal{H}) \hookrightarrow \mathcal{J}_{q_2}(\mathcal{H})$ holds if $1 \leq q_1 < q_2 \leq \infty$ [6]. In other words, if $A \in \mathcal{J}_{q_1}(\mathcal{H})$, then $A \in \mathcal{J}_{q_2}(\mathcal{H})$ and $\|A\|_{\mathcal{J}_{q_2}(\mathcal{H})} \leq \|A\|_{\mathcal{J}_{q_1}(\mathcal{H})}$.

Consider the following assumptions with $1 \leq q < \infty$:

- (A1) $\Pi_0 \in \mathcal{J}_q(\mathcal{H})$ and Π_0 is nonnegative.
- (A2) $Q(\cdot) \in L^1([0, t_f]; \mathcal{J}_q(\mathcal{H}))$ and $Q(t)$ is nonnegative for all $t \in [0, t_f]$.
- (A3) $\bar{\mathcal{C}}\bar{\mathcal{C}}^*(\cdot) \in L^\infty([0, t_f]; \mathcal{L}(\mathcal{H}))$ and $\bar{\mathcal{C}}\bar{\mathcal{C}}^*(t)$ is nonnegative for $t \in [0, t_f]$.

The existence of a mild solution of (12) is established in Lemma 2.3. The proof is omitted because the lemma follows directly from [6, Theorem 3.6].

Lemma 2.3 [6, Theorem 3.6] *Let \mathcal{H} be a separable Hilbert space. Suppose assumptions (A1)–(A3) hold. Then, the equation*

$$\begin{aligned} \Pi(t) = & \mathcal{S}(t)\Pi_0\mathcal{S}^*(t) + \int_0^t \mathcal{S}(t-\tau) \\ & (Q(\tau) - \Pi(\tau)\bar{\mathcal{C}}\bar{\mathcal{C}}^*(\tau)\Pi(\tau))\mathcal{S}^*(t-\tau)d\tau \end{aligned} \quad (13)$$

provides a unique mild solution to (12) in the space $L^2([0, t_f]; \mathcal{J}_{2q}(\mathcal{H}))$. The solution is in $C([0, t_f]; \mathcal{J}_q(\mathcal{H}))$ and is pointwise self-adjoint and nonnegative.

The covariance operator $\Pi(t)$ characterizes the uncertainty of the estimation error. The expected value of the squared norm of the estimation error is the trace of the covariance operator $\Pi(t)$ [7, 45]: $\text{Tr}(\Pi(t)) = \mathbb{E}[\|\mathcal{Z}(t) - \hat{\mathcal{Z}}(t)\|_{\mathcal{H}}^2]$.

The following assumption is vital to the main results in this paper:

- (A4) For each sensor $i \in \{1, 2, \dots, m_s\}$, the kernel of the output operator $\mathcal{C}_i(x, t)$ is continuous with respect to location $x \in \mathbb{R}^2$ [7, Definition 4.5]. That is, there exists a continuous function $l : \mathbb{R}^+ \rightarrow \mathbb{R}^+$ such that $l(0) = 0$ and $\|\mathcal{C}_i(x_1, t) - \mathcal{C}_i(x_2, t)\|_{L^2(\Omega)} \leq l(|x_1 - x_2|_2)$ for all $t \in [0, t_f]$ and all $x_1, x_2 \in \mathbb{R}^2$.

Assumption (A4) is important in that, roughly speaking, it establishes the continuity of the covariance operator with respect to sensor state (Lemma 2.5), which further permits the existence of a solution to the optimization problem proposed in this paper (Theorem 3.1), its finite-dimensional approximation (Theorem 4.1), and the convergence to the exact optimal cost of the approximate optimal cost (Theorem 4.2).

Remark 2.4 *The time invariant kernel in (8) is continuous with respect to location, where $l(u) = (4r_i c_0 u + u^2)^{1/2} / (4r_i^2)$ for sensor i in assumption (A4) for $c_0 > 0$.*

The sensors' locations determine where the output is measured and, furthermore, how the covariance operator evolves through (13). We characterize this relation by a composite mapping. Since the output operator $\mathcal{C}^*(\cdot, t)$ is a mapping of the sensors' locations at time t , the composite output operator $\bar{\mathcal{C}}\bar{\mathcal{C}}^*(\cdot)$ is a mapping of the sensor state in $[0, t_f]$ and so is $\Pi(\cdot)$ by (13), although the sensor state is not explicitly reflected in the notation of the latter two mappings. Hence, we can define the uncertainty cost $\int_0^{t_f} \text{Tr}(\Pi(t))dt$ as a mapping of the sensor state. Let $K : C([0, t_f]; \mathbb{R}^n) \rightarrow \mathbb{R}^+$ such that $K(\zeta) := \int_0^{t_f} \text{Tr}(\Pi(t))dt$. Lemma 2.5 below states the continuity of the uncertainty cost with respect to the sensor state. Its proof can be found in the supplementary material.

Lemma 2.5 *Let assumptions (A1)–(A3) hold with $q = 1$ and $\Pi \in C([0, t_f]; \mathcal{J}_1(\mathcal{H}))$ be defined in (13). If assumption (A4) holds, then the mapping $K(\cdot)$ is continuous.*

2.5 Finite-dimensional approximation

A finite-dimensional approximation of the infinite-dimensional state estimate $\hat{Z}(t)$ and covariance operator $\Pi(t)$ is necessary for numerical computation. Consider a finite-dimensional subspace $\mathcal{H}_N \subset \mathcal{H}$ with dimension N . The inner product and norm of \mathcal{H}_N are inherited from that of \mathcal{H} . Let $P_N : \mathcal{H} \rightarrow \mathcal{H}_N$ denote the orthogonal projection of \mathcal{H} onto \mathcal{H}_N . Let $\hat{Z}_N(t) := P_N \hat{Z}(t)$ and $S_N(t) := P_N \mathcal{S}(t) P_N$ be the finite-dimensional approximations of $\hat{Z}(t)$ and $\mathcal{S}(t)$, respectively. The approximated version of the estimation (10) is

$$\dot{\hat{Z}}_N(t) = A_N \hat{Z}_N(t) + \Pi_N(t) C_N(t) R^{-1} (y(t) - \hat{y}_N(t)), \quad (14)$$

$$\hat{y}_N(t) = C_N^*(t) \hat{Z}_N(t), \quad (15)$$

with initial condition $\hat{Z}_N(0) = P_N \hat{Z}_0$. The approximations $A_N \in \mathcal{L}(\mathcal{H}_N)$ and $C_N^*(t) \in \mathcal{L}(\mathcal{H}_N; \mathbb{R}^{m_s})$ are of \mathcal{A} and $\mathcal{C}^*(t)$, respectively, and $\Pi_N(t)$ is the finite-dimensional approximation of $\Pi(t)$ such that

$$\begin{aligned} \Pi_N(t) = & S_N(t) \Pi_{0,N} S_N^*(t) + \int_0^t S_N(t-\tau) (Q_N(\tau) \\ & - \Pi_N(\tau) \bar{C}_N \bar{C}_N^*(\tau) \Pi_N(\tau)) S_N^*(t-\tau) d\tau, \end{aligned} \quad (16)$$

where $\Pi_{0,N} := P_N \Pi_0 P_N$ and $Q_N(t) := P_N Q(t) P_N$ are approximations of Π_0 and $Q(t)$, respectively, and $\bar{C}_N \bar{C}_N^*(\tau)$ is short for $C_N R^{-1} C_N^*(\tau)$.

If the subspace \mathcal{H}_N is chosen such that it is spanned by the first N functions of the orthonormal basis $\{\phi_i\}_{i=1}^\infty$ that spans \mathcal{H} , then $\text{Tr}(\Pi_N(t)) = \text{Tr}(P_N \Pi(t) P_N) = \sum_{i=1}^N \langle \phi_i, \Pi(t) \phi_i \rangle$. To establish convergence of the approximate covariance operator $\Pi_N(\cdot)$ to the original operator $\Pi(\cdot)$, the following assumptions are made:

- (A5) Both Π_0 and sequence $\{\Pi_{0,N}\}_{N=1}^\infty$ are elements of $\mathcal{J}_q(\mathcal{H})$. Both Π_0 and $\Pi_{0,N}$ are nonnegative for all $N \in \mathbb{N}$ and $\|\Pi_0 - \Pi_{0,N}\|_{\mathcal{J}_q(\mathcal{H})} \rightarrow 0$ as $N \rightarrow \infty$.
- (A6) Both $Q(\cdot)$ and sequence $\{Q_N(\cdot)\}_{N=1}^\infty$ are elements of $L^1([0, t_f]; \mathcal{J}_q(\mathcal{H}))$. Both $Q(\tau)$ and $Q_N(\tau)$ are nonnegative for all $\tau \in [0, t_f]$ and all $N \in \mathbb{N}$ and satisfy $\int_0^t \|Q(\tau) - Q_N(\tau)\|_{\mathcal{J}_q(\mathcal{H})} d\tau \rightarrow 0$ for all $t \in [0, t_f]$ as $N \rightarrow \infty$.
- (A7) Both $\bar{C} \bar{C}^*(\cdot)$ and sequence $\{\bar{C}_N \bar{C}_N^*(\cdot)\}_{N=1}^\infty$ are elements of $L^\infty([0, t_f]; \mathcal{L}(\mathcal{H}))$. Both $\bar{C} \bar{C}^*(t)$ and $\bar{C}_N \bar{C}_N^*(t)$ are nonnegative for all N and $t \in [0, t_f]$. And $\text{ess sup}_{t \in [0, t_f]} \|\bar{C} \bar{C}^*(t) - \bar{C}_N \bar{C}_N^*(t)\|_{\text{op}} \rightarrow 0$ holds as $N \rightarrow \infty$ ($\|\cdot\|_{\text{op}}$ denotes the operator norm).

Note that assumptions (A1), (A2), and (A3) are contained within assumptions (A5), (A6), and (A7), respectively.

The convergence of the approximate covariance operator $\Pi_N(\cdot)$ is stated in the next theorem whose proof is omitted since the theorem is reproduced from [6, Theorem 3.5].

Theorem 2.6 ([6, Theorem 3.5]) *Suppose $\mathcal{S}(t)$ is a strongly continuous semigroup of linear operators over a Hilbert space \mathcal{H} and that $\{S_N(t)\}$ is a sequence of uniformly continuous semigroup over the same Hilbert space that satisfy*

$$\|\mathcal{S}(t)\phi - S_N(t)\phi\| \rightarrow 0, \quad \|\mathcal{S}^*(t)\phi - S_N^*(t)\phi\| \rightarrow 0 \quad (17)$$

as $N \rightarrow \infty$, uniformly in $[0, t_f]$ for each $\phi \in \mathcal{H}$. Suppose assumptions (A5)–(A7) hold. If $\Pi(\cdot) \in C([0, t_f]; \mathcal{J}_q(\mathcal{H}))$ is a solution of (13) and $\Pi_N(\cdot) \in C([0, t_f]; \mathcal{J}_q(\mathcal{H}))$ is the sequence of solution of (16), then $\sup_{t \in [0, t_f]} \|\Pi(t) - \Pi_N(t)\|_{\mathcal{J}_q(\mathcal{H})} \rightarrow 0$ as $N \rightarrow \infty$.

The following assumption and lemma are related to the continuity with respect to location of the approximate output kernel and the continuity with respect to sensor state of the trace of the approximate covariance operator, which are analogous to assumption (A4) and Lemma 2.5, respectively.

- (A8) The approximated input operator $C_{i,N}(x, t)$ is continuous with respect to location $x \in \mathbb{R}^2$, that is, there exists a continuous function $l_N : \mathbb{R}^+ \rightarrow \mathbb{R}^+$ such that $l_N(0) = 0$ and $\|C_{i,N}(x_1, t) - C_{i,N}(x_2, t)\|_{L^2(\Omega)} \leq l_N(|x_1 - x_2|_2)$ for all $t \in [0, t_f]$, all $x_1, x_2 \in \mathbb{R}^2$, and all $i \in \{1, 2, \dots, m_s\}$.

Similar to the mapping $K(\cdot)$ in Lemma 2.5, we can characterize the approximate uncertainty cost as a mapping of the sensor state ζ , where continuity is established in Lemma 2.7, whose proof is in the supplementary material.

Lemma 2.7 *Let assumptions (A5)–(A7) hold and $\Pi_N(t)$ be defined as in (16). If assumption (A8) holds, then the mapping $K_N : C([0, t_f]; \mathbb{R}^n) \rightarrow \mathbb{R}^+$ such that $K_N(\zeta) := \int_0^{t_f} \text{Tr}(\Pi_N(t)) dt$ is continuous.*

3 Problem formulation

We now introduce the formulation of the optimization problem. Given the dynamics and initial condition (2) of the sensors, the dynamics of the diffusion-advection process (6), and the second moment of the initial state noise $w_0(\cdot, \cdot)$, the process noise $w(\cdot, \cdot, t)$, and measurement noise $v(t)$, the problem below yields the optimal guidance for a team of mobile sensors to estimate a 2D diffusion-advection process.

The cost function consists of two parts: one part accounts for reducing the estimation uncertainty (*uncertainty cost*), and the other accounts for the motion of the sensors (*mobility cost*). The uncertainty cost is the integral of the trace of the covariance operator $\Pi(\cdot)$ over the horizon $[0, t_f]$, i.e., $\int_0^{t_f} \text{Tr}(\Pi(t))dt$. The mobility cost $J_m(\zeta, p)$ is defined as

$$J_m(\zeta, p) = \int_0^{t_f} h(\zeta(t), t) + g(p(t), t) dt + h_f(\zeta(t_f)). \quad (18)$$

Here, $h : \mathbb{R}^n \times [0, t_f] \rightarrow \mathbb{R}^+$ is a continuous function that characterizes the cost associated with the state of the mobile sensors. For example, a hazardous field can be modeled by h , where $h(\zeta(t), t)$ evaluates the exposure of the mobile sensors, which can shorten the sensor's life span. The cost of the guidance is characterized by $g : \mathbb{R}^m \times [0, t_f] \rightarrow \mathbb{R}^+$. For example, a quadratic guidance effort is $g(p(t), t) = p^\top(t)\gamma p(t)$, where $\gamma \in \mathbb{R}^{m \times m}$ is symmetric and positive definite. The guidance cost can address limited onboard resources, like fuel or batteries, by treating γ as the penalty coefficient. The terminal state cost $h_f : \mathbb{R}^n \rightarrow \mathbb{R}^+$ evaluates the cost associated with the terminal state. An exemplary scenario is when the sensors are expected to come close to a set of pre-assigned terminal locations $x_f \in \Omega^{m_s}$, where $h_f(\zeta(t_f)) := |M\zeta(t_f) - x_f|_2^2$.

The motion of the sensors follows from the dynamics (2), which constrain the optimization. Denote the admissible set of guidance functions as $\mathcal{P} := L^2([0, t_f]; P)$, where P is the set of admissible guidance (values) defined at the end of Section 2.2.

The optimization problem is formulated as follows:

$$\begin{aligned} & \underset{p \in \mathcal{P}}{\text{minimize}} && \int_0^{t_f} \text{Tr}(\Pi(t)) + h(\zeta(t), t) + g(p(t), t) dt \\ & && + h_f(\zeta(t_f)) \\ & \text{subject to} && \dot{\zeta}(t) = a\zeta(t) + bp(t), \quad \zeta(0) = \zeta_0, \end{aligned} \quad (\text{P})$$

where $\Pi(t)$ is given by (13) with a given initial condition $\Pi(0) = \Pi_0$. It suffices to search for guidance p that minimizes the cost of (P), because the sensor state ζ is entirely determined by guidance p via the sensor dynamics and the given initial condition ζ_0 , which further determines $\Pi(\cdot)$ through (13) with a given initial covariance $\Pi(0)$.

A special case is considered in [10] where only a quadratic guidance effort is considered in the mobility cost. Such a formulation applies to the case of limited onboard resources of each mobile sensor when γ is diagonal. It minimizes the Lagrangian function of the optimization problem that minimizes the uncertainty cost subject to the constraints of bounded guidance effort and linear dynamics of the mobile sensors.

The following three assumptions are necessary for the existence of a solution to problem (P).

- (A9) The set of admissible guidance $P \subset \mathbb{R}^m$ is closed and convex.
- (A10) The mappings $h : \mathbb{R}^n \times [0, t_f] \rightarrow \mathbb{R}^+$, $g : \mathbb{R}^m \times [0, t_f] \rightarrow \mathbb{R}^+$, and $h_f : \mathbb{R}^n \rightarrow \mathbb{R}^+$ are continuous. For every $t \in [0, t_f]$, the function $g(p, t)$ is convex about p .
- (A11) There exists a constant $d_1 > 0$ with $g(p, t) \geq d_1 |p|_2^2$ for all $(p, t) \in P \times [0, t_f]$.

Assumptions (A9)–(A11) are generally met in applications with real vehicles. Assumption (A9) is satisfied when the values of admissible guidance vary along a continuum. The continuity requirement in assumption (A10) on the cost functions h , g , and h_f is typically satisfied. And the convexity requirement in assumption (A10) and quadratic boundedness from below in assumption (A11) can be met if g is quadratic in p , e.g., $g(p, t) = p^\top(t)\gamma(t)p(t)$ for a symmetric and positive definite matrix $\gamma(t)$ (which is continuous with respect to t) such that d_1 can be chosen as the minimum eigenvalue of $\gamma(t)$ for $t \in [0, t_f]$ (see [3, Corollary VI.1.6]).

Theorem 3.1 below states the existence of a solution to problem (P), whose proof can be found in Appendix A.

Theorem 3.1 *Consider problem (P) and let assumptions (A1)–(A4) and (A9)–(A11) hold. Then problem (P) has a solution.*

We use Pontryagin's minimum principle to characterize an optimal solution of (P). Consider the Hamiltonian

$$\begin{aligned} H(\zeta(t), p(t), \lambda(t), t) &= \text{Tr}(\Pi(t)) \\ &+ h(\zeta(t), t) + g(p(t), t) + \lambda^\top(t)(a\zeta(t) + bp(t)), \end{aligned} \quad (19)$$

where $\lambda(t) \in \mathbb{R}^n$ is the costate associated with $\zeta(t)$. The necessary conditions of (local) optimality are as follows:

$$\dot{\zeta}^*(t) = a\zeta^*(t) + bp^*(t), \quad (20a)$$

$$\zeta^*(0) = \zeta_0, \quad (20b)$$

$$\begin{aligned} \dot{\lambda}^*(t) &= -a^\top \lambda^*(t) - \nabla_\zeta h(\zeta^*(t), t) \\ &\quad - \nabla_\zeta \text{Tr}(\Pi^*(t)), \end{aligned} \quad (20c)$$

$$\lambda^*(t_f) = \nabla_\zeta h_f(\zeta^*(t_f)), \quad (20d)$$

$$0 = \nabla_p g(p^*(t), t) + b^\top \lambda^*(t), \quad (20e)$$

where $\Pi^*(\cdot)$ is evaluated along the optimal system state $\zeta^*(\cdot)$ and we use the first-order necessary condition $\nabla_p H(\zeta^*(t), p^*(t), \lambda^*(t), t) = 0$ in (20e) for H to attain its minimum at $p^*(t)$. The necessary condition (20) essentially requires the solution to a two-point boundary value problem, which further requires the derivation of $\nabla_\zeta \text{Tr}(\Pi^*(t))$. We refer to a similar derivation in [7], where the gradient of the covariance operator's trace

with respect to sensor's guidance is taken. The i th row of $\nabla_{\zeta}\text{Tr}(\Pi^*(t))$, denoted by $[\nabla_{\zeta}\text{Tr}(\Pi^*(t))]_i$, is the partial derivative of $\text{Tr}(\Pi^*(t))$ with respect to the i th element of the state $\zeta^*(t)$ for $i \in \{1, 2, \dots, n\}$. Since trace is a linear operator, we have

$$[\nabla_{\zeta}\text{Tr}(\Pi^*(t))]_i = \frac{\partial\text{Tr}(\Pi^*(t))}{\partial[\zeta(t)]_i} = \text{Tr}\left(\frac{\partial\Pi^*(t)}{\partial[\zeta(t)]_i}\right). \quad (21)$$

By the chain rule, (21) becomes

$$\text{Tr}\left(\frac{\partial\Pi^*(t)}{\partial[\zeta(t)]_i}\right) = \text{Tr}(D_{\bar{C}\bar{C}^*(t)}\Pi^*(t) \circ D_{[\zeta(t)]_i}\bar{C}\bar{C}^*(t)), \quad (22)$$

where $D_{\bar{C}\bar{C}^*(t)}\Pi(t)$ is the Fréchet derivative of the Riccati operator with respect to the composite output operator $\bar{C}\bar{C}^*(t)$ and $D_{[\zeta(t)]_i}\bar{C}\bar{C}^*(t)$ is the Fréchet derivative of $\bar{C}\bar{C}^*(t)$ with respect to $[\zeta(t)]_i$. Denote $D_{\bar{C}\bar{C}^*(t)}\Pi^*(t)$ by $\Lambda(t)$ and, by [7, Theorem 5.5], $\Lambda(t)$ is the unique solution to

$$\begin{aligned} \Lambda h(t) = & - \int_0^t \mathcal{S}(t-s)((\Lambda h)(s)\bar{C}\bar{C}^*(s)\Pi(s) \\ & + \Pi(s)\bar{C}\bar{C}^*(s)(\Lambda h)(s) \\ & + \Pi(s)h(s)\Pi(s))\mathcal{S}^*(t-s)ds \end{aligned} \quad (23)$$

with $\Lambda(0) = 0$ for all $h \in C([0, t_f]; \mathcal{J}_1(\mathcal{H}))$ and all $t \in [0, t_f]$. The approximated version of problem (P) and the two-point boundary value problem (20) will be applied to solve for optimal guidance in Section 4.

4 Solving optimal guidance using approximation

Since the infinite-dimensional terms in (P) have to be approximated for computation as introduced in Section 2.5, we arrive at the approximated problem:

$$\begin{aligned} \text{minimize}_{p_N \in \mathcal{P}} \quad & \int_0^{t_f} \text{Tr}(\Pi_N(t)) + h(\zeta(t), t) + g(p_N(t), t)dt \\ & + h_f(\zeta(t_f)) \\ \text{subject to} \quad & \dot{\zeta}(t) = a\zeta(t) + bp_N(t), \quad \zeta(0) = \zeta_0, \end{aligned} \quad (\text{AP})$$

where $\Pi_N(t)$ is obtained through (16). It suffices to search for guidance p_N , because both the sensor state ζ and the approximated estimation covariance Π_N are fully determined by the guidance and initial conditions. The existence of a solution of problem (AP) is guaranteed in Theorem 4.1 with the proof in Appendix B.

Theorem 4.1 *Consider problem (AP) and let assumptions (A5)–(A11) hold. Then problem (AP) has a solution.*

Solving problem (AP) provides a candidate solution, de-

noted by p_N^* , where N is the dimension of the approximation. The candidate p_N^* may not equal the exact optimal solution, denoted by p^* , of the original problem (P). However, as we show in the following theorem, the candidate p_N^* yields the optimal value of (AP) arbitrarily close to the one of (P), as the dimension N goes to infinity. Moreover, when p_N^* is evaluated in the original problem (P), the resulting cost is arbitrarily close to the optimal cost of (P).

Before we state this convergence result, we introduce an assumption on the set of admissible guidance functions.

(A12) There exist $p_{\max} > 0$ and $a_{\max} > 0$ such that the set of admissible guidance is $\mathcal{P}(p_{\max}, a_{\max}) := \{p \in C([0, t_f]; P) : |p(t)| \text{ is uniformly bounded by } p_{\max} \text{ and } |p(t_1) - p(t_2)| \leq a_{\max}|t_1 - t_2|, \forall t_1, t_2 \in [0, t_f]\}$.

Notice that the set $\mathcal{P}(p_{\max}, a_{\max})$ is sequentially compact, due to the Arzelà-Ascoli Theorem [35], since the guidance functions in $\mathcal{P}(p_{\max}, a_{\max})$ are uniformly equicontinuous and uniformly bounded. The parameters p_{\max} and a_{\max} may be determined by the vehicles carrying sensors. For example, p_{\max} and a_{\max} refer to the maximum speed and maximum acceleration, respectively, in the case of single integrator dynamics where p is the velocity command.

Theorem 4.2 below states the convergence of the approximation with the proof in Appendix C.

Theorem 4.2 *Consider problem (P) and its finite-dimensional approximation (AP). Let assumptions (A4)–(A12) hold and let p^* and p_N^* denote the optimal guidance of (P) and (AP), respectively. Then*

$$\lim_{N \rightarrow \infty} |J_{(\text{AP})}^*(p_N^*) - J_{(\text{P})}^*(p^*)| = 0. \quad (24)$$

Furthermore, the cost function of (P) evaluated at the guidance p_N^* converges to the optimal cost of (P)

$$\lim_{N \rightarrow \infty} |J_{(\text{P})}(p_N^*) - J_{(\text{P})}^*(p^*)| = 0. \quad (25)$$

Remark 4.3 *Two implications follow from the convergence result in Theorem 4.2. First, the convergence in (24) affirms the usage of approximation since the optimal cost of the approximate problem (AP) gets arbitrarily close to that of the exact problem (P) as the approximation gets finer. Second, the convergence in (25) affirms the optimal guidance computed using approximation. When the approximate optimal guidance is evaluated by the cost function of the original problem (P), the resulting value is arbitrarily close to the optimal cost of (P) as the approximation gets finer. In other words, the approximate optimal guidance is a sufficiently accurate proxy for the exact optimal guidance.*

Remark 4.4 *Assumptions are made for the existence of a solution to problem (P) ((A9)–(A11)), well-posedness of the Riccati operators ((A1)–(A4)), and the convergence of the approximated solution ((A5)–(A8) and (A12)). Assumptions (A9)–(A11) are regarding the mobility cost and the set of admissible guidance, which are generally satisfied in engineering applications (see the discussion in [11] before Theorem 3.1). The rest of the assumptions are typically satisfied with the diffusion-advection equation and Galerkin approximation (using eigenfunctions of the Laplacian operator). Details of how to check similar assumptions for the dual control problem can be found in [11, Section 4.1].*

The convergence stated in Theorem 4.2 is established based on several earlier stated results, including

- (1) the output operator’s continuity with respect to location (assumption (A4)), which leads to the continuity of the uncertainty cost with respect to sensor state (Lemma 2.5);
- (2) existence of the Riccati operator (Lemma 2.3) and convergence of its approximation (Theorem 2.6); and
- (3) sequential compactness of the set of admissible guidance functions (assumption (A12)), which leads to the continuity of the cost function with respect to guidance (Lemma C.1 in the Appendix).

Notice that these key results, in an analogous manner, are also required in [45] when establishing the convergence to the exact optimal sensor locations of the approximate optimal locations [45, Theorem 4.3], i.e.,

- (1) continuity with respect to location and compactness of the output operator (dual of [29, Theorem 2.10]), which lead to continuity of the Riccati operator with respect to sensor locations [45, Theorem 4.1];
- (2) existence of the Riccati operator [45, Theorem 2.5] and the convergence of its approximation [45, Theorem 4.2]; and
- (3) sequential compactness of the set of admissible locations, which is inherited from the setting that the spatial domain is closed and bounded in a finite-dimensional space.

To compute an optimal solution to problem (AP), we use Pontryagin’s minimum principle, which introduces a Hamiltonian function that has the same form as (19) except that the covariance operator $\Pi(t)$ in (19) is replaced by its approximation $\Pi_N(t)$. And correspondingly, the resulting two-point boundary value problem has the same form as (20) except for $\Pi(t)$ being replaced by $\Pi_N(t)$.

Remark 4.5 *The optimal sensor trajectory ζ^* steered by the optimal guidance p^* may be used as the reference*

trajectory tracked by the vehicle’s lower-level control. Although collision avoidance among the sensors is not discussed in this paper, it can be incorporated into the lower-level control using numerous methods in the existing literature, e.g., [42] and the references therein.

5 Simulation results

This section shows the simulation results obtained using the solution method proposed in Section 4. Comparison and analysis are made regarding the performance of the mobile sensor(s) under optimal guidance for the case of a single sensor, a team of homogeneous sensors, and a team of heterogeneous sensors.

We use the Galerkin scheme to approximate the infinite-dimensional terms. The orthonormal set of eigenfunctions of the Laplacian operator ∇^2 (with zero Dirichlet boundary condition) over the spatial domain $\Omega = [0, 1] \times [0, 1]$ is $\phi_{i,j}(x, y) = 2 \sin(\pi i x) \sin(\pi j y)$. With a single index $k := (i - 1)N + j$ such that $\phi_k := \phi_{i,j}$, the set of eigenfunctions $\{\phi_k\}_{k=1}^{N^2}$ spans an N^2 -dimensional space that is previously denoted by \mathcal{H}_N . For the orthogonal projection $P_N : \mathcal{H} \rightarrow \mathcal{H}_N$, it follows that $P_N^* = P_N$ and $P_N^* P_N \rightarrow I$ strongly. And the assumption (17) in Theorem 2.6 holds uniformly for all $t \in [0, t_f]$ as $N \rightarrow \infty$ [6]. We set p_{\max} and a_{\max} to be sufficiently large so that the solution is in the set $\mathcal{P}(p_{\max}, a_{\max})$. We plot the optimal cost $J_{(\text{AP})}^*(p_N^*)$ for N from 7 to 20, as shown in Fig. 1. The optimal cost shows a tendency of exponential convergence as we increase the number of basis functions. And we choose $N = 12$ in the rest of the simulations since it is the smallest dimension with the optimal cost within 1% of the optimal cost evaluated with the maximum dimension $N = 20$ in the trials.

The parameters in the simulation are $t_f = 2$, and $a = 0.01$. We use single integrator dynamics for each sensor. The state ζ is the 2D location of the sensors and guidance p is the 2D velocity command. In some applications, the flow field \mathbf{v} of the diffusion-advection process can affect the mobile sensors. For example, surface vehicles that measure the concentration of certain chemical substances or biological entities in a water body are subject to the movement of the water. Considering this realistic condition, we append the flow field $\mathbf{v} = [0.1, -0.1]^\top$ of advection to the right-hand side of the single integrator dynamics, which means the sensors will drift along the flow when zero guidance is implemented. The previous statements and results on the existence of solution and convergence of the approximate solution still hold within this setting. The optimization will find optimal guidance subject to (or possibly taking advantage of) this flow field. The sensor has the square-shaped average output kernel (see (8)) with $r_i = 0.05$, in which case its footprint covers only 1% of the domain in area.

We set $g(p(t)) = \gamma p^\top(t)p(t)/2$ and $h(\zeta(t), t) =$

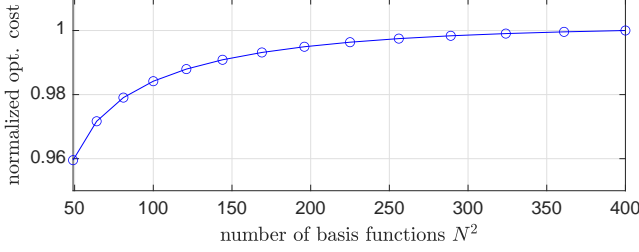


Fig. 1. Approximate optimal costs $J_{(\text{AP})}^*(p_N^*)$ normalized with respect to the optimal cost for $N^2 = 400$.

$h_f(\zeta(t_f)) = 0$ as the mobility cost, which is simply the quadratic guidance effort for $\gamma > 0$.

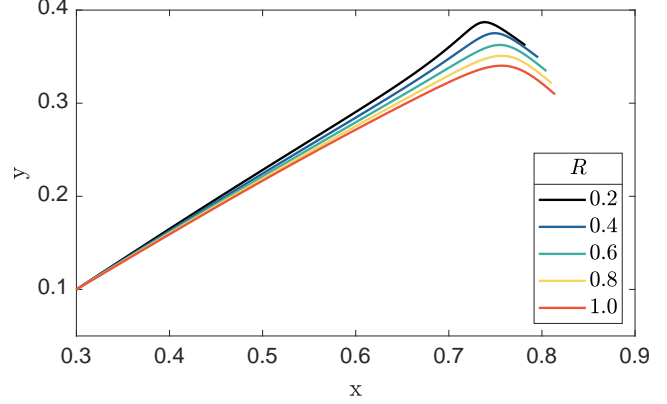
Assumption (A4) holds for the choice of output operator (see Remark 2.4). With the Galerkin approximation using the orthonormal eigenfunctions $\{\phi_k\}_{k=1}^{N^2}$, it can be shown that assumption (A8) holds for $l_N(\cdot) = N^2 l(\cdot)$. Assumptions (A5)–(A7) hold with $q = 1$ under the Galerkin approximation with aforementioned basis functions $\{\phi_k\}_{k=1}^{N^2}$ [6]. Assumptions (A9)–(A11) and (A12) hold for the choice of functions in the mobility cost and parameters of the set of admissible guidance functions, respectively.

To evaluate the performance of the optimal guidance in simulation, we set the deterministic portion of the initial condition of the PDE to zero, i.e., $\hat{Z}_0 = 0$, which excludes the bias from choosing a particular non-zero one. The stochastic portion of the initial condition w_0 is chosen as a zero-mean Gaussian process with non-stationary kernel function $k_0 : \Omega \times \Omega \rightarrow \mathbb{R}^+$ such that $k_0(x_1, x_2) := 9\exp(-|x_{12}|_2^2/200 - |x_{10}|_2^2/10 - |x_{20}|_2^2/10)$, where $x_{ij} := x_i - x_j$ for $i, j \in \{0, 1, 2\}$ and $x_0 \in \Omega$ represents the peak of the uncertainty in the domain and we set $x_0 = [0.75, 0.25]^\top$. For the state noise $w(t)$, we use a zero-mean Gaussian process with a homogeneous kernel function $k : \Omega \times \Omega \rightarrow \mathbb{R}^+$ such that $k(x_1, x_2) = \exp(-|x_{12}|_2^2/2000)$.

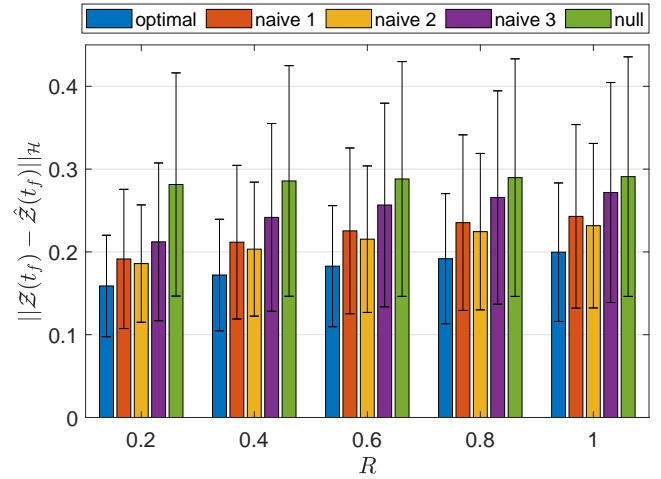
We use the forward-backward sweep method [27] to solve the two-point boundary problem (20) (with Π replaced by Π_N) and subsequently compute the optimal guidance. A fixed-step length of 0.01 and a relative tolerance of 1×10^{-6} are applied in the iterative procedure. The forward propagation of (20a) and (16) and the backward propagation of (20c) are computed via the Runge-Kutta method.

5.1 Single sensor results

Two important parameters in the problem setting are the sensor noise variance R and mobility penalty γ . Smaller R yields higher sensor quality, whereas smaller γ yields better mobility of the vehicle. For example, if γ is the mass of the vehicle, then the guidance effort is



(a) Optimal trajectories for various values of the sensor noise variance R

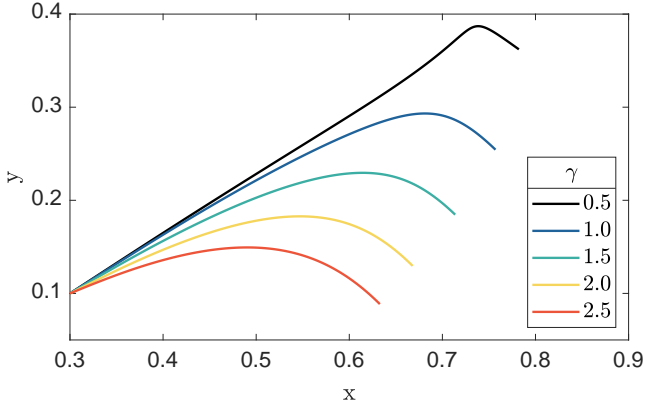


(b) Norm of the terminal estimation error for various values of sensor noise variance R . The color bar shows the mean value; the error bar shows the standard deviation.

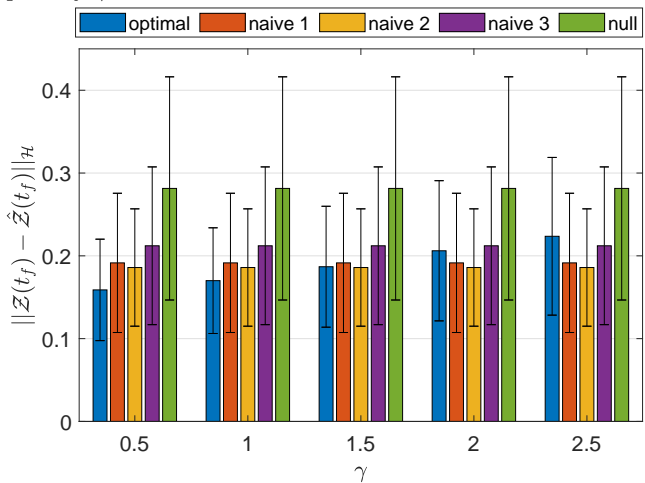
Fig. 2. The value of mobility penalty γ is fixed at 0.5, whereas the sensor noise's variance R takes values in the set $\{0.2, 0.4, 0.6, 0.8, 1\}$.

the kinetic energy of the vehicle. These parameters affect the performance of the estimation as shown next. In this simulation, the sensor is initiated at $\zeta_0 = [0.3, 0.1]^\top$. Monte Carlo simulations of 100 trials compare the optimal guidance with three naive guidance policies as follows: naive 1 crosses the domain by reaching the opposite of the initial location within domain at $[0.7, 0.9]^\top$ at a constant speed; naive 2 reaches the peak of the initial uncertainty x_0 at a constant speed; and naive 3 circulates the domain in the clockwise direction with center $[0.5, 0.5]^\top$, radius $1/\sqrt{5}$, and angular speed π rad/s. A stationary sensor is also included for comparison whose null guidance merely compensates for the flow field \mathbf{v} .

First, hold either R or γ fixed and vary the other to observe the variation of the optimal trajectory. Fig. 2a displays the trajectories when $\gamma = 0.5$ and R varies from 0.2 to 1. The sensor maneuvers less as R increases, which



(a) Optimal trajectories for various values of the mobility penalty γ



(b) Norm of the terminal estimation error for various values of the mobility penalty γ . The color bar shows the mean value; the error bar shows the standard deviation.

Fig. 3. The value of sensor noise’s variance R is fixed at 0.2, whereas the mobility penalty γ takes values in the set $\{0.5, 1, 1.5, 2, 2.5\}$.

indicates the optimal guidance’s compensation for deteriorating sensor quality by moving it closer to the peak of the initial uncertainty at $x_0 = [0.75, 0.25]^\top$.

For the Monte Carlo trials, the mean and standard deviation of the terminal estimation error’s norm are shown in Fig. 2b. The optimal guidance exhibits smaller mean and variance of terminal estimation error over the naive guidance policies and the null guidance at each evaluated R . Notice that the advantage is preserved when the sensor quality deteriorates as R increases.

Fig. 3a displays the trajectories when $R = 0.2$ and γ varies from 0.5 to 2.5. A bigger value of γ suppresses the guidance effort and hence reduces the range of the sensor’s motion. The results of Monte Carlo trials when γ varies are shown in Fig. 3b. Notice that the mean and standard deviation are invariant for each naive guidance

policy and the null guidance among the varying γ since the sensor trajectory steered by each of these guidance policies is independent of γ . The optimal guidance shows its advantage over the other guidance policies at a relatively smaller values of γ , e.g., at 0.5 and 1. This advantage is gradually lost as γ takes relatively bigger values, e.g., 2 and 2.5. This comparison suggests that the optimal guidance may not be the best option for vehicles with large γ (e.g., when the vehicle is heavy), despite the fact that the guidance is still optimal for the chosen cost function in simulation.

Fig. 4 shows the snapshots of the sensor trajectory under the optimal guidance and contour plot of the pointwise variance of the estimation error among the Monte Carlo trials with $\gamma = 1$ and $R = 0.2$. The pointwise variance is computed at each point in a uniform grid of 144×144 sampling points in the domain Ω . The sensor is steered quickly towards the area with higher uncertainty near $[0.75, 0.25]^\top$ (see the snapshot at $t = 0.8$ s). Eventually, the sensor starts to drift along the flow field $\mathbf{v} = [0.1, -0.1]^\top$ (see the snapshot at $t = 2$ s). That sensor can effectively reduce the uncertainty of the estimation error as can be observed from the drop in the pointwise variance in the sensor’s footprint. Note that the zero Dirichlet boundary condition also contributes to reducing the uncertainty of the estimation error via diffusion and advection.

5.2 Team of homogeneous sensors

To demonstrate the framework’s capability in guiding a team of multiple sensors, we simulate four homogeneous sensors ($R = 0.2, \gamma = 0.5$). To adapt to a total of four sensors, the kernel functions for w_0 and w are set to be $4k_0(x_1, x_2)$ and $4k(x_1, x_2)$, respectively, and the peak of the initial uncertainty is set to the center $[0.5, 0.5]^\top$. The other settings are identical to those in Section 5.1. Fig. 5 shows the snapshots of the sensors’ trajectories under the optimal guidance and contour plot of the pointwise variance of the estimation error among the Monte Carlo trials. Similar to the case of a single sensor in Fig. 4, the sensors quickly sweep the peak of the initial uncertainty in the center and expand to cover the domain (see the snapshot at $t = 0.6$ s). The pointwise variance drops along sensors’ footprints. The sensors essentially drift along the flow to reduce the guidance effort (see the snapshot at $t = 2$ s).

5.3 Team of heterogeneous sensors

The parameters R and γ essentially relate to operational planning: one may invest more for better sensor quality or a swifter vehicle. Consequently, one would necessarily invest more for a team of superior mobile sensors (e.g., $R = 0.2$ and $\gamma = 0.5$) than a team of poor mobile sensors (e.g., $R = 1$ and $\gamma = 2.5$). The latter has five times as much sensor noise (in terms of standard deviation) and

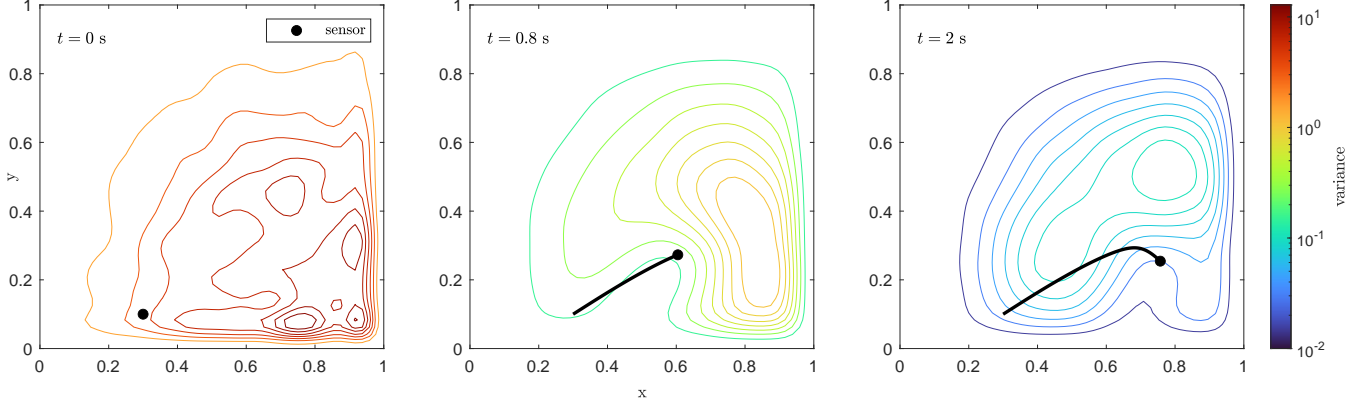


Fig. 4. Trajectory of the sensor following the optimal guidance. The contours represent the level curves of pointwise variance of the estimation error on a uniform grid within the domain, computed from the Monte Carlo simulations.

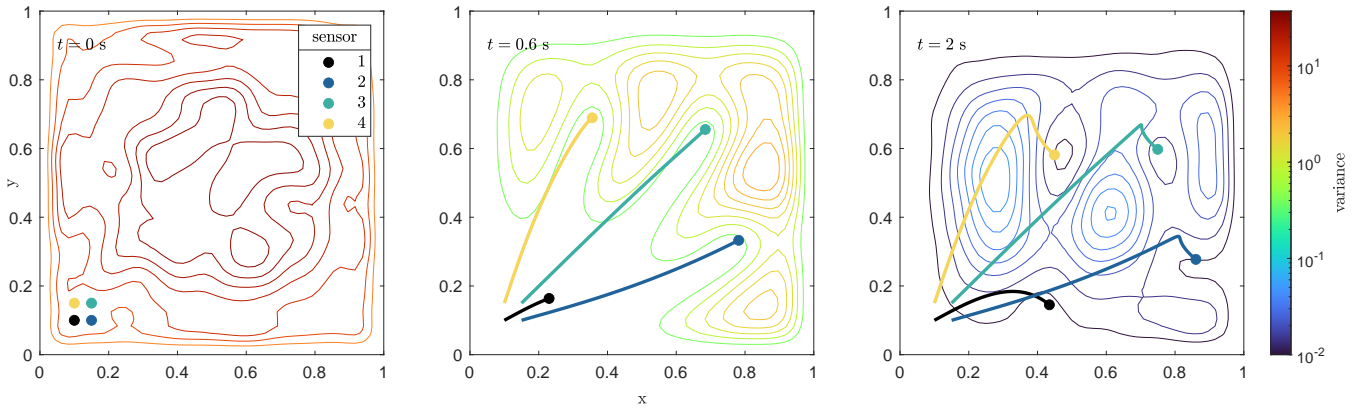


Fig. 5. Trajectories of multiple homogeneous sensors following the optimal guidance. The contours represent the level curves of pointwise variance of the estimation error on a uniform grid within the domain.

five times the mobility penalty as the former. One may balance the conflicting needs of performance and investment by deploying a team of heterogeneous sensors, i.e., a mixed team of superior and poor sensors.

The following simulation compares the performance of a team of heterogeneous sensors (including m_p poor sensors and $8 - m_p$ superior sensors, for m_p in the range of $\{1, 2, \dots, 7\}$) with that of homogeneous teams ($m_p = 0$ for superior sensors only and $m_p = 8$ for poor sensors only). The sensors are initiated in the lower left corner of the domain. To adapt to a total of eight sensors, the kernel functions for w_0 and w are set to be $8k_0(x_1, x_2)$ and $8k(x_1, x_2)$, respectively, and the peak of the initial uncertainty is set to the center of the domain at $[0.5, 0.5]^T$. Fig. 6 shows the normalized optimal total cost and uncertainty cost for the heterogeneous team compared with homogeneous teams of superior and poor sensors. The performance deteriorates judged by the rising costs as the number of poor sensors increases in team. However, the degradation of the heterogeneous team (when $m_p \leq 5$) is maintained within 20% of the superior team in both the total cost and uncertainty cost, which indicates the cost effectiveness of the heterogeneous team

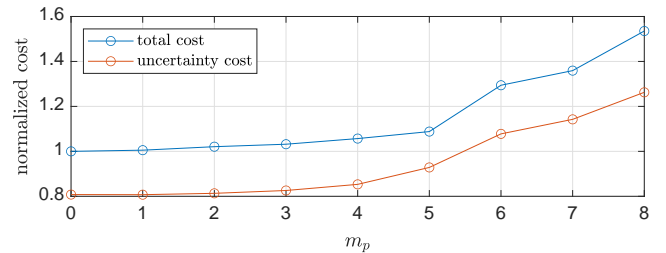


Fig. 6. Normalized optimal total cost and uncertainty cost of a heterogeneous team with m_p poor sensors and $8 - m_p$ superior sensors.

since the investment reduces linearly as m_p increases.

6 Conclusion

This paper proposes a guidance design method for a team of mobile sensors to estimate a spatiotemporal process modeled by a 2D diffusion-advection process. We formulate an optimization problem that minimizes the sum of the trace of the covariance operator of the Kalman-Bucy filter and a generic mobility cost of the sensors subject to the dynamics of the sensor platforms.

Conditions for the existence of a solution to the proposed problem are established, where a fundamental assumption is that the output kernel is continuous with respect to location. Approximation of the infinite-dimensional terms permits the computation of the optimal guidance, and we prove that the approximated problem's optimal cost converges to that of the exact problem. Moreover, we prove that the optimal guidance obtained from an approximate problem yields the cost evaluated by the exact problem's cost function arbitrarily close to the exact optimal cost. Exponential convergence in the optimal cost can be observed in simulations when the approximation dimension increases.

We use Pontryagin's minimum principle to numerically compute optimal guidance. The numerical solutions are evaluated in simulations. We study how the optimal trajectory and terminal estimation error change subject to the varying values of sensor noise variance and the mobility penalty for a single sensor. Trajectories of the sensors and the evolution of the pointwise variance are shown for a single sensor and a homogeneous team of sensors in a flow field. We also study the cost-effectiveness of a heterogeneous team of mixed sensors with superior and poor qualities by comparing the performance degradation to that of the homogeneous team of superior sensors.

Ongoing and future work includes establishing a convergence rate in Theorem 4.2, incorporating constraints to the problem formulation (e.g., constraints on sensor states), extension to more complicated sensor dynamics (e.g., control-affine), and demonstrating the framework experimentally using a swarm of quadrotor helicopters in an outdoor testbed.

Acknowledgments

The authors would like to thank the reviewers for their helpful suggestions. Work reported in this article was sponsored under a seed grant from Northrop Grumman.

A Proof of Theorem 3.1

Since we have proved that the uncertainty cost $\int_0^{t_f} \text{Tr}(\Pi(t))dt$ is a continuous mapping $K(\cdot)$ of the sensor state ζ (see Lemma 2.5), the existence of optimal guidance of (P) can be proved using the techniques of proving existence of solution to an optimal control (guidance) problem.

Proof of Theorem 3.1 Without loss of generality, we consider the case of one mobile sensor, i.e., $m_s = 1$. The case of $m_s \geq 2$ follows naturally.

Our proof follows the proof in [43, Chapter 6.2] which proves existence of a solution to an optimal control problem based on functional analytic theorems. Consider

problem (P)'s admissible set of guidance functions $\mathcal{P} := \{p \in L^2([0, t_f]; \mathbb{R}^m) : p(t) \in P, t \in [0, t_f]\}$. Since there exists $p_0 \in \mathcal{P}$ such that $J_{(P)}(p_0) < \infty$ (e.g., $p_0 = 0$ that yields a stationary sensor at ζ_0), let $\mathcal{P}_0 := \{p \in \mathcal{P} : J_{(P)}(p) \leq J_{(P)}(p_0)\}$.

Condition-1: The set \mathcal{P}_0 is bounded.

Condition-2: The set \mathcal{P}_0 is weakly sequentially closed.

Condition-3: The mapping $J_{(P)}(\cdot) : \mathcal{P} \rightarrow \mathbb{R}^+$ is weakly sequentially lower semicontinuous on \mathcal{P}_0 .

Condition-1 and Condition-2 imply that \mathcal{P}_0 is weakly sequentially compact. By [43, Theorem 6.1.4], problem (P) has a solution when Condition-1–Condition-3 hold.

Before showing these three conditions, we first define the solution map $T : L^2([0, t_f]; \mathbb{R}^m) \rightarrow C([0, t_f]; \mathbb{R}^n)$ of the sensor dynamics (2) by $(Tp)(t) := \zeta(t) = e^{\alpha t} \zeta_0 + \int_0^t e^{\alpha(t-\tau)} \beta p(\tau) d\tau$ for $t \in [0, t_f]$. The continuity of the map T is straightforward [43], i.e., there exists $c_4 > 0$ such that $\|Tp\|_{C([0, t_f]; \mathbb{R}^n)} \leq c_4 \|p\|_{L^2([0, t_f]; \mathbb{R}^m)}$.

Proof of Condition-1: Suppose $p \in \mathcal{P}_0$, then

$$\begin{aligned} J_{(P)}(p_0) &\geq J_{(P)}(p) \\ &= \int_0^{t_f} h(Tp(t), t) + g(p(t), t) + \text{Tr}(\Pi(t)) dt \\ &\quad + h_f(Tp(t_f)) \\ &\geq \int_0^{t_f} d_1 |p(t)|^2 dt \\ &= d_1 \|p\|_{L^2([0, t_f]; \mathbb{R}^m)}^2. \end{aligned} \tag{A.1}$$

Since $d_1 > 0$, the boundedness of \mathcal{P}_0 follows.

Proof of Condition-2: Suppose $\{p_k\} \subset \mathcal{P}_0$ and $\{p_k\}$ converges to p weakly (denoted by $p_k \rightharpoonup p$). We wish to show $p \in \mathcal{P}_0$. We start with establishing that \mathcal{P} is weakly sequentially closed and, hence, $p \in \mathcal{P}$. Subsequently, we show $J_{(P)}(p) \leq J_{(P)}(p_0)$ to conclude Condition-2.

To show that the set \mathcal{P}_0 is weakly sequentially closed, by [39, Theorem 2.11], it suffices to show that \mathcal{P} is closed and convex. Let $\{q_k\} \subset \mathcal{P}$ and $q_k \rightarrow q$. We want to show $q \in \mathcal{P}$, i.e., $q \in L^2([0, t_f]; \mathbb{R}^m)$ and $q(t) \in P$ for $t \in [0, t_f]$. Since $L^2([0, t_f]; \mathbb{R}^m)$ is complete, we can choose a subsequence $\{q_{k_j}\} \subset \mathcal{P}$ that converges to q pointwise almost everywhere on $[0, t_f]$ [44, p. 53]. Since P is closed (assumption (A9)), $q(t) \in P$ for almost all $t \in [0, t_f]$. Hence, \mathcal{P} is closed. The convexity of \mathcal{P} follows from that of P (assumption (A9)), i.e., if $p_1, p_2 \in \mathcal{P}$, then $\lambda p_1 + (1-\lambda)p_2 \in L^2([0, t_f]; \mathbb{R}^m)$ and $\lambda p_1(t) + (1-\lambda)p_2(t) \in P$ for $t \in [0, t_f]$ and $\lambda \in [0, 1]$.

What remain to be shown is $J_{(P)}(p) \leq J_{(P)}(p_0)$. Since $p_k \rightharpoonup p$, by definition, we have $Tp_k \rightarrow Tp$. We now

show that the sequence $\{Tp_k\}$ contains a uniformly convergent subsequence in $C([0, t_f]; \mathbb{R}^n)$. The sequence $\{Tp_k\} \subset C([0, t_f]; \mathbb{R}^n)$ is uniformly bounded and uniformly equicontinuous for the following reasons: Since $\|Tp_k\|_{C([0, t_f]; \mathbb{R}^n)} \leq c_4 \|p_k\|_{L^2([0, t_f]; \mathbb{R}^m)}$, it follows that $\|Tp_k\|_{C([0, t_f]; \mathbb{R}^n)}$ is uniformly bounded, because $\{p_k\} \subset \mathcal{P}_0$ which is a bounded set. For $s, t \in [0, t_f]$, we have

$$\begin{aligned} |Tp_k(s) - Tp_k(t)|_1 &= \left| \int_s^t \alpha Tp_k(\tau) + \beta p_k(\tau) d\tau \right|_1 \\ &\leq |t - s| |\alpha|_1 \|Tp_k\|_{C([0, t_f]; \mathbb{R}^n)} \\ &\quad + |t - s|^{1/2} |\beta|_2 \|p_k\|_{L^2([0, t_f]; \mathbb{R}^m)}. \end{aligned}$$

Since $\{\|p_k\|_{L^2([0, t_f]; \mathbb{R}^m)}\}$ and $\{\|Tp_k\|_{C([0, t_f]; \mathbb{R}^n)}\}$ both are uniformly bounded for all $p_k \in \mathcal{P}_0$, $\{Tp_k\}$ is uniformly equicontinuous. By the Arzelà-Ascoli Theorem [35], there is a uniformly convergent subsequence $\{Tp_{k_j}\} \subset \{Tp_k\}$. Without loss of generality, we assume $p_k \rightarrow p$ and $Tp_k \rightarrow Tp$ uniformly on $[0, t_f]$, and $J_{(P)}(p_k) \leq J_{(P)}(p_0)$. We have

$$\begin{aligned} &J_{(P)}(p_0) - J_{(P)}(p) \\ &= J_{(P)}(p_0) - J_{(P)}(p_k) + J_{(P)}(p_k) - J_{(P)}(p) \\ &\geq J_{(P)}(p_k) - J_{(P)}(p). \end{aligned} \quad (\text{A.2})$$

Hence, to show $J_{(P)}(p) \leq J_{(P)}(p_0)$, it suffices to show $J_{(P)}(p) \leq \liminf_{k \rightarrow \infty} J_{(P)}(p_k)$, which is to show

$$\begin{aligned} &h_f(Tp(t_f)) + \int_0^{t_f} h(Tp(t), t) + g(p(t), t) + \text{Tr}(\Pi(t)) dt \\ &\leq \liminf_{k \rightarrow \infty} h_f(Tp_k(t_f)) + \int_0^{t_f} h(Tp_k(t), t) + g(p_k(t), t) \\ &\quad + \text{Tr}(\Pi^k(t)) dt, \end{aligned} \quad (\text{A.3})$$

where $\Pi^k(t)$ is the solution of (13) associated with sensor state Tp_k . Since $\{Tp_k\}$ converges to Tp uniformly on $[0, t_f]$, the continuity of $h_f(\cdot)$ implies

$$h_f(Tp(t_f)) = \liminf_{k \rightarrow \infty} h_f(Tp_k(t_f)); \quad (\text{A.4})$$

Fatou's lemma [35] implies

$$\int_0^{t_f} h(Tp(t), t) dt \leq \liminf_{k \rightarrow \infty} \int_0^{t_f} h(Tp_k(t), t) dt; \quad (\text{A.5})$$

and Lemma 2.5 implies

$$\int_0^{t_f} \text{Tr}(\Pi(t)) dt = \liminf_{k \rightarrow \infty} \int_0^{t_f} \text{Tr}(\Pi^k(t)) dt. \quad (\text{A.6})$$

To prove (A.3), based on (A.4)–(A.6), it suffices to show

$$\int_0^{t_f} g(p(t), t) dt \leq \liminf_{k \rightarrow \infty} \int_0^{t_f} g(p_k(t), t) dt. \quad (\text{A.7})$$

By contradiction, assume there is $\lambda > 0$ such that

$$\liminf_{k \rightarrow \infty} \int_0^{t_f} g(p_k(t), t) dt < \lambda < \int_0^{t_f} g(p(t), t) dt. \quad (\text{A.8})$$

There exists a subsequence $\{p_{k_j}\} \subset \{p_k\}$ such that $\{p_{k_j}\} \subset O_\lambda = \{q \in L^2([0, t_f]; \mathbb{R}^m) : \int_0^{t_f} g(q(t), t) dt \leq \lambda\}$. We wish to show that O_λ is weakly sequentially closed. By [43, Theorem 6.1.5], it suffices to show that O_λ is convex and closed. Since $g(\cdot, t) : \mathbb{R}^m \rightarrow \mathbb{R}$ is convex for all $t \in [0, t_f]$, it follows that O_λ is convex. Let $\{q_k\} \subset O_\lambda$ and $\|q_k - q\|_{L^2([0, t_f]; \mathbb{R}^m)}$ converges to 0 as $k \rightarrow \infty$. We can choose a subsequence $\{q_{k_j}\} \subset \{q_k\}$ such that q_{k_j} converges to q pointwise almost everywhere on $[0, t_f]$ [44, p. 53]. Now we have $g(q_{k_j}(t), t) \geq 0$ for all $t \in [0, t_f]$ (assumption (A11)) and $\lim_{j \rightarrow \infty} g(q_{k_j}(t), t) = g(q(t), t)$ almost everywhere on $[0, t_f]$. By Fatou's lemma [35], $\int_0^{t_f} g(q(t), t) dt \leq \liminf_{k \rightarrow \infty} \int_0^{t_f} g(q_{k_j}(t), t) dt \leq \lambda$, where the last inequality holds due to the fact that $\{q_{k_j}\} \subset O_\lambda$. Hence, $q \in O_\lambda$ and O_λ is closed.

Since O_λ is weakly sequentially closed, $p_{k_j} \rightarrow p$ implies that $p \in O_\lambda$, which contradicts (A.8). Hence, $J_{(P)}(p) \leq J_{(P)}(p_0)$ is proved, and we conclude Condition-2.

Proof of Condition-3: We now show that the mapping $J_{(P)}(\cdot) : \mathcal{P} \rightarrow \mathbb{R}$ is weakly sequentially lower semicontinuous on \mathcal{P}_0 . Suppose $\{p_k\} \subset \mathcal{P}_0$ and $p_k \rightarrow p \in \mathcal{P}_0$. We wish to establish $J_{(P)}(p) \leq \liminf_{k \rightarrow \infty} J_{(P)}(p_k)$, which can be shown using the technique of proving Condition-2 (starting from (A.3)).

Thus we conclude the existence of a solution of problem (P). \square

B Proof of Theorem 4.1

Proof Since $\text{Tr}(\Pi_N(t)) \geq 0$ ($\Pi_N(t)$ is nonnegative and self-adjoint for all $t \in [0, t_f]$) and the mapping $K_N : C([0, t_f]; \mathbb{R}^n) \rightarrow \mathbb{R}$ is continuous (see Lemma 2.5), the proof is analogous to that of Theorem 3.1, where $\Pi(t)$ is replaced by $\Pi_N(t)$. \square

C Proof of Theorem 4.2

Recall that the notation $J_{(\text{AP})}^*(p_N^*)$ means the optimal value of (AP) evaluated at its optimal solution p_N^* , where the dimension of approximation applied to (AP) is N (as indicated by the subscript of p_N^*). In this section, we attach a subscript to (AP), such as $J_{(\text{AP})_N}(p)$, to indicate its dimension when it is not reflected by the argument, e.g., $J_{(\text{AP})_N}(p)$ means that the cost of (AP) using an N -dimensional approximation evaluated at a guidance function p . Lemma C.1 (see proof in the supplementary material) will be used in the proof of Theorem 4.2.

Lemma C.1 Consider problems (P) and its approximation (AP). Let assumptions (A4)–(A12) hold. Then the following results hold:

1. For $p \in C([0, t_f]; \mathbb{R}^m)$, $\lim_{N \rightarrow \infty} J_{(\text{AP})_N}(p) = J_{(\text{P})}(p)$;
2. The mapping $J_{(\text{P})} : C([0, t_f]; \mathbb{R}^m) \rightarrow \mathbb{R}^+$ such that $J_{(\text{P})}(p) = \int_0^{t_f} \text{Tr}(\Pi(t)) dt + J_m(\zeta, p)$ is continuous, where ζ is the sensor state steered by p under the dynamics (2) and $\Pi(\cdot)$ is the covariance operator obtained through (13) with sensor state ζ .

Proof of Theorem 4.2 We start with proving (24), i.e., $|J_{(\text{AP})}^*(p_N^*) - J_{(\text{P})}^*(p^*)| \rightarrow 0$ as $N \rightarrow \infty$. First,

$$\begin{aligned} J_{(\text{AP})}^*(p_N^*) &= \min_{p \in \mathcal{P}(p_{\max}, a_{\max})} J_{(\text{AP})_N}(p) \\ &\leq J_{(\text{AP})_N}(p^*) \\ &\leq |J_{(\text{AP})_N}(p^*) - J_{(\text{P})}^*(p^*)| + J_{(\text{P})}^*(p^*). \end{aligned}$$

It follows that

$$\limsup_{N \rightarrow \infty} J_{(\text{AP})}^*(p_N^*) \leq J_{(\text{P})}^*(p^*), \quad (\text{C.1})$$

because $|J_{(\text{AP})_N}(p^*) - J_{(\text{P})}^*(p^*)| \rightarrow 0$ as $N \rightarrow \infty$ (see Lemma C.1-1).

To proceed with proving (24), in addition to (C.1), we shall show $\liminf_{N \rightarrow \infty} J_{(\text{AP})}^*(p_N^*) \geq J_{(\text{P})}^*(p^*)$. Choose a convergent subsequence $\{J_{(\text{AP})}^*(p_{N_k}^*)\}_{k=1}^\infty$ such that

$$\lim_{k \rightarrow \infty} J_{(\text{AP})}^*(p_{N_k}^*) = \liminf_{N \rightarrow \infty} J_{(\text{AP})}^*(p_N^*). \quad (\text{C.2})$$

Since the subsequence $\{p_{N_k}^*\}_{k=1}^\infty \subset \mathcal{P}(p_{\max}, a_{\max})$ which is uniformly equicontinuous and uniformly bounded, by the Arzelà-Ascoli Theorem [35], there is a (uniformly) convergent subsequence of $\{p_{N_k}^*\}_{k=1}^\infty$. We denote this convergent subsequence with the same indices $\{N_k\}_{k=1}^\infty$ to simplify notation. Denote the limit of $\{p_{N_k}^*\}_{k=1}^\infty$ by p_{inf}^* , i.e.,

$$\lim_{k \rightarrow \infty} \|p_{N_k}^* - p_{\text{inf}}^*\|_{C([0, t_f]; \mathbb{R}^m)} = 0. \quad (\text{C.3})$$

Next, we show

$$\lim_{k \rightarrow \infty} |J_{(\text{AP})}^*(p_{N_k}^*) - J_{(\text{P})}^*(p_{\text{inf}}^*)| = 0. \quad (\text{C.4})$$

First notice that for all $p \in \mathcal{P}(p_{\max}, a_{\max})$, $J_{(\text{AP})_N}(p)$ converges to $J_{(\text{P})}(p)$ pointwise as the dimension of approximation N goes to infinity (see Lemma C.1-1). Furthermore, since the sequence of approximated uncertainty cost $\{\int_0^{t_f} \text{Tr}(\Pi_N(t)) dt\}_{N=1}^\infty$ is a monotonically

increasing sequence, the sequence $\{J_{(\text{AP})_N}(p)\}_{N=1}^\infty$ is a monotonically increasing sequence for each p on the compact set $\mathcal{P}(p_{\max}, a_{\max})$. By Dini's Theorem [36, Theorem 7.13], $|J_{(\text{AP})_N}(p) - J_{(\text{P})}(p)| \rightarrow 0$ uniformly on $\mathcal{P}(p_{\max}, a_{\max})$ as $N \rightarrow \infty$. By Moore-Osgood Theorem [36, Theorem 7.11], this uniform convergence and the convergence $p_{N_k}^* \rightarrow p_{\text{inf}}^*$ as $k \rightarrow \infty$ (see (C.3)) imply that

$$\lim_{k \rightarrow \infty} J_{(\text{P})}(p_{N_k}^*) = \lim_{j \rightarrow \infty} \lim_{k \rightarrow \infty} J_{(\text{AP})_j}^*(p_{N_k}^*). \quad (\text{C.5})$$

And the iterated limit in (C.5) equals the double limit [38, p. 140], i.e.,

$$\begin{aligned} \lim_{j \rightarrow \infty} \lim_{k \rightarrow \infty} J_{(\text{AP})_j}^*(p_{N_k}^*) &= \lim_{j \rightarrow \infty} J_{(\text{AP})_j}^*(p_{N_k}^*) \\ &= \lim_{k \rightarrow \infty} J_{(\text{AP})}^*(p_{N_k}^*). \end{aligned} \quad (\text{C.6})$$

By (C.5), (C.6), and the fact that $J_{(\text{P})}(p_{\text{inf}}^*) = \lim_{k \rightarrow \infty} J_{(\text{P})}(p_{N_k}^*)$ holds (due to the continuity of $J_{(\text{P})}(\cdot)$, see Lemma C.1-2), we conclude that (C.4) holds and

$$\begin{aligned} \liminf_{N \rightarrow \infty} J_{(\text{AP})}^*(p_N^*) &= \lim_{k \rightarrow \infty} J_{(\text{AP})}^*(p_{N_k}^*) \\ &= J_{(\text{P})}(p_{\text{inf}}^*) \\ &\geq J_{(\text{P})}^*(p^*). \end{aligned} \quad (\text{C.7})$$

Therefore, we conclude $\lim_{N \rightarrow \infty} J_{(\text{AP})}^*(p_N^*) = J_{(\text{P})}^*(p^*)$ from (C.1) and (C.7).

Next, we prove (25), i.e., $|J_{(\text{P})}(p_N^*) - J_{(\text{P})}^*(p^*)| \rightarrow 0$ as $N \rightarrow \infty$. We start with $J_{(\text{P})}^*(p^*) \leq J_{(\text{P})}(p_N^*)$ for all N , which implies that

$$J_{(\text{P})}^*(p^*) \leq \liminf_{N \rightarrow \infty} J_{(\text{P})}(p_N^*). \quad (\text{C.8})$$

To prove (25), what remains to be shown is $J_{(\text{P})}^*(p^*) \geq \limsup_{N \rightarrow \infty} J_{(\text{P})}(p_N^*)$. Choose a convergent subsequence $\{J_{(\text{P})}(p_{N_j}^*)\}_{j=1}^\infty$ such that $\lim_{j \rightarrow \infty} J_{(\text{P})}(p_{N_j}^*) = \limsup_{N \rightarrow \infty} J_{(\text{P})}(p_N^*)$. Since $\{p_{N_j}^*\}_{j=1}^\infty \subset \mathcal{P}(p_{\max}, a_{\max})$ is uniformly equicontinuous and uniformly bounded, by Arzelà-Ascoli Theorem [35], $\{p_{N_j}^*\}_{j=1}^\infty$ has a (uniformly) convergent subsequence which we denote with the same indices $\{N_j\}_{j=1}^\infty$ to simplify notation. Denote the limit of $\{p_{N_j}^*\}_{j=1}^\infty$ by p_{sup}^* such that

$$\lim_{j \rightarrow \infty} \|p_{N_j}^* - p_{\text{sup}}^*\|_{C([0, t_f]; \mathbb{R}^m)} = 0. \quad (\text{C.9})$$

Due to the continuity of $J_{(\text{P})}(\cdot)$ (see Lemma C.1-1), we have $J_{(\text{P})}(p_{\text{sup}}^*) = \lim_{j \rightarrow \infty} J_{(\text{P})}(p_{N_j}^*) = \limsup_{N \rightarrow \infty} J_{(\text{P})}(p_N^*)$.

Now we have

$$\begin{aligned}
& J_{(P)}(p_{\text{sup}}^*) \\
& \leq |J_{(P)}(p_{\text{sup}}^*) - J_{(P)}^*(p^*)| + J_{(P)}^*(p^*) \\
& = |J_{(P)}(p_{\text{sup}}^*) - \lim_{N \rightarrow \infty} J_{(\text{AP})}^*(p_N^*)| + J_{(P)}^*(p^*) \\
& = |J_{(P)}(p_{\text{sup}}^*) - \lim_{j \rightarrow \infty} J_{(\text{AP})}^*(p_{N_j}^*)| + J_{(P)}^*(p^*). \quad (\text{C.10})
\end{aligned}$$

Since the sequence of approximated uncertainty cost $\{\int_0^{t_f} \Pi_N(t) dt\}_{N=1}^\infty$ is a monotonically increasing sequence, the sequence $\{J_{(\text{AP})_N}(p)\}_{N=1}^\infty$ is a monotonically increasing sequence for each p on the compact set $\mathcal{P}(p_{\text{max}}, a_{\text{max}})$. Since $\lim_{N \rightarrow \infty} J_{(\text{AP})_N}(p) = J_{(P)}(p)$ for all $p \in \mathcal{P}(p_{\text{max}}, a_{\text{max}})$ (see Lemma C.1-1), by Dini's Theorem [36, Theorem 7.13], the limit holds uniformly on $\mathcal{P}(p_{\text{max}}, a_{\text{max}})$ as $N \rightarrow \infty$. By Moore-Osgood Theorem [36, Theorem 7.11], this uniform convergence and the convergence $p_{N_j}^* \rightarrow p_{\text{sup}}^*$ as $j \rightarrow \infty$ (see (C.9)) imply that $J_{(P)}(p_{\text{sup}}^*) = \lim_{k \rightarrow \infty} \lim_{j \rightarrow \infty} J_{(\text{AP})_k}^*(p_{N_j}^*)$. Furthermore, the iterated limit equals the double limit [38, p. 140], i.e.,

$$\begin{aligned}
\lim_{k \rightarrow \infty} \lim_{j \rightarrow \infty} J_{(\text{AP})_k}^*(p_{N_j}^*) & = \lim_{j \rightarrow \infty} J_{(\text{AP})_k}^*(p_{N_j}^*) \\
& = \lim_{j \rightarrow \infty} J_{(\text{AP})}^*(p_{N_j}^*). \quad (\text{C.11})
\end{aligned}$$

Hence, $J_{(P)}(p_{\text{sup}}^*) = \lim_{j \rightarrow \infty} J_{(\text{AP})}^*(p_{N_j}^*)$, which, combined with (C.10), implies

$$J_{(P)}^*(p^*) \geq J_{(P)}(p_{\text{sup}}^*) = \limsup_{N \rightarrow \infty} J_{(P)}(p_N^*). \quad (\text{C.12})$$

The desired convergence $\lim_{N \rightarrow \infty} J_{(P)}(p_N^*) = J_{(P)}^*(p^*)$ follows from (C.8) and (C.12). \square

References

- [1] A. Bensoussan. *Filtrage optimal des systèmes linéaires*. Dunod, 1971.
- [2] A. Bensoussan. Optimization of sensors' location in a distributed filtering problem. In *Stability of Stochastic Dynamical Systems. Lecture Notes in Mathematics*, volume 294, pages 62–84. Springer, 1972.
- [3] R. Bhatia. *Matrix Analysis*, volume 169. Springer Science & Business Media, 1996.
- [4] R. S. Bucy and P. D. Joseph. *Filtering for stochastic processes with applications to guidance*, volume 326. American Mathematical Soc., 2005.
- [5] J. Burns, E. Cliff, C. Rautenberg, and L. Zietsman. Optimal sensor design for estimation and optimization of PDE systems. In *Proc. 2010 American Control Conf.*, pages 4127–4132.
- [6] J. A. Burns and C. N. Rautenberg. Solutions and approximations to the Riccati integral equation with values in a space of compact operators. *SIAM J. Control Optim.*, 53(5):2846–2877, 2015.
- [7] J. A. Burns and C. N. Rautenberg. The infinite-dimensional optimal filtering problem with mobile and stationary sensor networks. *Numer. Funct. Anal. Optim.*, 36(2):181–224, 2015.
- [8] J. A. Burns, E. W. Sachs, and L. Zietsman. Mesh independence of Kleinman-Newton iterations for Riccati equations in Hilbert space. *SIAM J. Control Optim.*, 47(5):2663–2692, 2008.
- [9] L. Carotenuto, P. Muraca, and G. Raiconi. Optimal location of a moving sensor for the estimation of a distributed-parameter process. *Int. J. Control*, 46(5):1671–1688, 1987.
- [10] S. Cheng and D. A. Paley. Optimal guidance and estimation of a 1D diffusion process by a team of mobile sensors. In *Proc. 59th Conf. Decision and Control*, pages 1222–1228, 2020.
- [11] S. Cheng and D. A. Paley. Optimal control of a 2D diffusion-advection process with a team of mobile actuators under jointly optimal guidance. *Automatica*, 133:109866, 2021.
- [12] M. A. Demetriou. Gain adaptation and sensor guidance of diffusion PDEs using on-line approximation of optimal feedback kernels. In *Proc. 2016 American Control Conf.*, pages 2536–2541.
- [13] M. A. Demetriou. Guidance of mobile actuator-plus-sensor networks for improved control and estimation of distributed parameter systems. *IEEE Trans. Automat. Control*, 55(7):1570–1584, 2010.
- [14] M. A. Demetriou. Adaptive control of 2-D PDEs using mobile collocated actuator/sensor pairs with augmented vehicle dynamics. *IEEE Trans. Automatic Control*, 57(12):2979–2993, 2012.
- [15] M. A. Demetriou. Incorporating impact of hazardous and toxic environments on the guidance of mobile sensor networks used for the cooperative estimation of spatially distributed processes. In *Proc. 57th Conf. Decision and Control*, pages 1317–1322, 2018.
- [16] M. A. Demetriou. Using modified Centroidal Voronoi Tessellations in kernel partitioning for optimal actuator and sensor selection of parabolic PDEs with static output feedback. In *Proc. 56th Conf. Decision and Control*, pages 3119–3124, 2018.
- [17] M. A. Demetriou and N. A. Gatsonis. Scheduling of static sensor networks and management of mobile sensor networks for the detection and containment of moving sources in spatially distributed processes. In *Proc. 17th Mediterranean Conf. Control and Automation*, pages 187–192, 2009.
- [18] M. A. Demetriou and I. I. Hussein. Estimation of spatially distributed processes using mobile spatially distributed sensor network. *SIAM J. Control Optim.*, 48(1):266–291, 2009.
- [19] Z. Emirsjlow and S. Townley. From PDEs with boundary control to the abstract state equation with an unbounded input operator: A tutorial. *Euro. J. Control*, 6(1):27–49, 2000.
- [20] W. Hu, K. Morris, and Y. Zhang. Sensor location in a controlled thermal fluid. In *Proc. 55th Conf. Decision and Control*, pages 2259–2264, 2016.
- [21] L. Imsland. Partially distributed optimization for mobile sensor path-planning. In *Proc. 56th Conf. Decision and Control*, pages 3101–3106, 2017.
- [22] R. E. Kalman. A New Approach to Linear Filtering and Prediction Problems. *J. Basic Engineering*, 82(1):35–45, 03 1960.
- [23] D. Karagiannis and V. Radisavljevic-Gajic. A backstepping boundary observer for a simply supported beam. *IEEE Trans. Automat. Control*, 64(9):3809–3816, 2019.

- [24] A. Khapalov. L^∞ -exact observability of the heat equation with scanning pointwise sensor. *SIAM J. Control Optim.*, 32(4):1037–1051, 1994.
- [25] A. Y. Khapalov. Continuous observability for parabolic system under observations of discrete type. *IEEE Trans. Automat. Control*, 38(9):1388–1391, 1993.
- [26] G. B. Lamont and K. S. Kumar. State estimation in distributed parameter systems via least squares and invariant embedding. *J. Math. Anal. Appl.*, 38(3):588–606, 1972.
- [27] M. McAsey, L. Mou, and W. Han. Convergence of the forward-backward sweep method in optimal control. *Comput. Optim. Appl.*, 53(1):207–226, 2012.
- [28] J. S. Meditch. Least-squares filtering and smoothing for linear distributed parameter systems. *Automatica*, 7(3):315–322, 1971.
- [29] K. Morris. Linear-quadratic optimal actuator location. *IEEE Trans. Automat. Control*, 56(1):113–124, 2010.
- [30] K. Morris and S. Yang. Comparison of actuator placement criteria for control of structures. *J. Sound and Vibration*, 353:1–18, 2015.
- [31] K. A. Morris. Optimal output estimation for infinite-dimensional systems with disturbances. *Systems and Control Letters*, 146:104803, 2020.
- [32] S. J. Moura and H. K. Fathy. Optimal boundary control & estimation of diffusion-reaction PDEs. In *Proc. 2011 American Control Conf.*, pages 921–928.
- [33] S. Omatu and J. H. Seinfeld. *Distributed parameter systems: theory and applications*. Clarendon Press, 1989.
- [34] Y. Privat, E. Trélat, and E. Zuazua. Optimal shape and location of sensors for parabolic equations with random initial data. *Arch. Ration. Mech. Anal.*, 216(3):921–981, 2015.
- [35] H. Royden and P. Fitzpatrick. Real analysis (4th edition). *New Jersey: Printice-Hall Inc*, 2010.
- [36] W. Rudin. *Principles of mathematical analysis*, volume 3. McGraw-Hill New York, 1964.
- [37] A. Smyshlyaev and M. Krstic. Backstepping observers for a class of parabolic PDEs. *Systems and Control Letters*, 54(7):613–625, 2005.
- [38] A. E. Taylor. *General theory of functions and integration*. Courier Corporation, 1985.
- [39] F. Tröltzsch. *Optimal control of partial differential equations: theory, methods, and applications*, volume 112. American Mathematical Soc., 2010.
- [40] D. W. Veldman, R. H. Fey, H. J. Zwart, M. M. Van De Wal, J. D. Van Den Boom, and H. Nijmeijer. Sensor and actuator placement for proportional feedback control in advection-diffusion equations. *IEEE Control Systems Letters*, 4(1):193–198, 2020.
- [41] J. W. Wang, Y. Q. Liu, Y. Y. Hu, and C. Y. Sun. A spatial domain decomposition approach to distributed H^∞ observer design of a linear unstable parabolic distributed parameter system with spatially discrete sensors. *Int. J. Control*, 90(12):2772–2785, 2017.
- [42] L. Wang, A. D. Ames, and M. Egerstedt. Safety barrier certificates for collisions-free multirobot systems. *IEEE Trans. Robotics*, 33(3):661–674, 2017.
- [43] J. Werner. *Optimization theory and applications*. Springer-Verlag, 2013.
- [44] K. Yosida. *Functional analysis*, volume 123. springer, 1988.
- [45] M. Zhang and K. Morris. Sensor choice for minimum error variance estimation. *IEEE Trans. Automat. Control*, 63(2):315–330, 2018.

Supplementary material for: Optimal guidance and estimation of a 2D diffusion-advection process by a team of mobile sensors[★]

Sheng Cheng^a, Derek A. Paley^b

^a *University of Illinois Urbana-Champaign*

^b *University of Maryland, College Park*

Abstract

This supplement provides proofs for Lemmas 2.5, 2.7, and C.1 in [2].

Key words: Infinite-dimensional systems; Multi-agent systems; Modeling for control optimization; Guidance navigation and control.

Lemma 2.5 *Let assumptions (A1)–(A3) hold with $q = 1$ and $\Pi \in C([0, t_f]; \mathcal{J}_1(\mathcal{H}))$ be defined in [2, (13)]. If assumption (A4) holds, then the mapping $K(\cdot)$ is continuous.*

Proof Without loss of generality, consider the case of one mobile sensor, i.e., $m_s = 1$. The case of multiple sensors follows naturally. We first show a consequence of the output operator \mathcal{C}^* being continuous with respect to location. Consider two sensor states $\zeta_1, \zeta_2 \in C([0, t_f]; \mathbb{R}^n)$. For any $\phi \in \mathcal{H} = L^2(\Omega)$ and all $t \in [0, t_f]$,

$$\begin{aligned} & \|\mathcal{C}^*(M\zeta_1(t), t)\phi - \mathcal{C}^*(M\zeta_2(t), t)\phi\| \\ & \leq \|\mathcal{C}(M\zeta_1(t), t) - \mathcal{C}(M\zeta_2(t), t)\|_{L^2(\Omega)} \|\phi\|_{L^2(\Omega)} \\ & \leq l(|M(\zeta_1(t) - \zeta_2(t))|_2) \|\phi\|_{L^2(\Omega)}, \end{aligned} \quad (1)$$

where we use the fact that $\mathcal{C}(\cdot, \cdot)$ is the integral kernel of $\mathcal{C}^*(\cdot, \cdot)$. Hence,

$$\begin{aligned} & \|\mathcal{C}^*(M\zeta_1(t), t) - \mathcal{C}^*(M\zeta_2(t), t)\|_{\mathcal{L}(\mathcal{H}; \mathbb{R})} \\ & \leq l(|M(\zeta_1(t) - \zeta_2(t))|_2). \end{aligned} \quad (2)$$

Since \mathbb{R} is finite-dimensional, there exists $c_1 > 0$ such

[★] This paper was not presented at any IFAC meeting. Corresponding author Sheng Cheng.

Email addresses: chengs@illinois.edu (Sheng Cheng), dpaley@umd.edu (Derek A. Paley).

that [1, proof of Lemma 4.3]

$$\begin{aligned} & \|\mathcal{C}^*(M\zeta_1(t), t) - \mathcal{C}^*(M\zeta_2(t), t)\|_{\mathcal{J}_1(\mathcal{H}; \mathbb{R})} \\ & \leq c_1 \|\mathcal{C}^*(M\zeta_1(t), t) - \mathcal{C}^*(M\zeta_2(t), t)\|_{\mathcal{L}(\mathcal{H}; \mathbb{R})}. \end{aligned} \quad (3)$$

For brevity, we shall use $\mathcal{C}_1(t)$ for $\mathcal{C}(M\zeta_1(t), t)$ and $\mathcal{C}_2(t)$ for $\mathcal{C}(M\zeta_2(t), t)$. Now,

$$\begin{aligned} & \|\mathcal{C}_1(t)R^{-1}\mathcal{C}_1^*(t) - \mathcal{C}_2(t)R^{-1}\mathcal{C}_2^*(t)\|_{\mathcal{J}_1(\mathcal{H})} \\ & \leq \|\mathcal{C}_1(t)R^{-1}\|_{\mathcal{J}_1(\mathbb{R}; \mathcal{H})} \|\mathcal{C}_1^*(t) - \mathcal{C}_2^*(t)\|_{\mathcal{J}_1(\mathcal{H}; \mathbb{R})} \\ & \quad + \|R^{-1}\mathcal{C}_2^*(t)\|_{\mathcal{J}_1(\mathcal{H}; \mathbb{R})} \|\mathcal{C}_1(t) - \mathcal{C}_2(t)\|_{\mathcal{J}_1(\mathbb{R}; \mathcal{H})} \\ & = \left(\|\mathcal{C}_1(t)R^{-1}\|_{\mathcal{J}_1(\mathbb{R}; \mathcal{H})} + \|R^{-1}\mathcal{C}_2^*(t)\|_{\mathcal{J}_1(\mathcal{H}; \mathbb{R})} \right) \\ & \quad \|\mathcal{C}_1^*(t) - \mathcal{C}_2^*(t)\|_{\mathcal{J}_1(\mathcal{H}; \mathbb{R})} \\ & \leq c_2 \|\mathcal{C}_1^*(t) - \mathcal{C}_2^*(t)\|_{\mathcal{J}_1(\mathcal{H}; \mathbb{R})} \\ & \leq c_2 c_1 l(|M(\zeta_1(t) - \zeta_2(t))|_2) \end{aligned} \quad (4)$$

for some $c_2 > 0$, where the last inequality follows from (2) and (3).

By [2, (13)], the mapping $\Pi : [0, t_f] \rightarrow \mathcal{J}_1(\mathcal{H})$ varies continuously in $\sup_{t \in [0, t_f]} \|\cdot\|_{\mathcal{J}_1(\mathcal{H})}$ -norm with respect to $\tilde{\mathcal{C}}\mathcal{C}^*(\cdot)$ [1]. Hence, there exists $c_3 > 0$ such that

$$\sup_{t \in [0, t_f]} \|\Pi_1(t) - \Pi_2(t)\|_{\mathcal{J}_1(\mathcal{H})}$$

$$\leq \sup_{t \in [0, t_f]} c_3 \left\| \bar{C}_1 \bar{C}_1^*(t) - \bar{C}_2 \bar{C}_2^*(t) \right\|_{\mathcal{J}_1(\mathcal{H})}. \quad (5)$$

Now, we have

$$\begin{aligned} & |K(\zeta_1) - K(\zeta_2)| \\ &= \left| \int_0^{t_f} \|\Pi_1(t)\|_{\mathcal{J}_1(\mathcal{H})} - \|\Pi_2(t)\|_{\mathcal{J}_1(\mathcal{H})} dt \right| \\ &\leq \int_0^{t_f} \left| \|\Pi_1(t)\|_{\mathcal{J}_1(\mathcal{H})} - \|\Pi_2(t)\|_{\mathcal{J}_1(\mathcal{H})} \right| dt \\ &\leq \int_0^{t_f} \|\Pi_1(t) - \Pi_2(t)\|_{\mathcal{J}_1(\mathcal{H})} dt \\ &\leq \sup_{t \in [0, t_f]} \|\Pi_1(t) - \Pi_2(t)\|_{\mathcal{J}_1(\mathcal{H})} t_f. \end{aligned} \quad (6)$$

It follows from (4)–(6) that

$$|K(\zeta_1) - K(\zeta_2)| \leq c_1 c_2 c_3 t_f \sup_{t \in [0, t_f]} l(|M(\zeta_1(t) - \zeta_2(t))|_2),$$

and we conclude the continuity of $K(\cdot)$. \square

Lemma 2.7 *Let assumptions (A5)–(A7) hold and $\Pi_N(t)$ be defined as in [2, (16)]. If assumption (A8) holds, then the mapping $K_N : C([0, t_f]; \mathbb{R}^n) \rightarrow \mathbb{R}^+$ such that $K_N(\zeta) := \int_0^{t_f} \text{Tr}(\Pi_N(t)) dt$ is continuous.*

Proof Since the norm defined on \mathcal{H}_N is inherited from that of \mathcal{H} , the proof follows from the derivation of Lemma 2.5’s proof. \square

Lemma C.1 *Consider problems [2, (P)] and its approximation [2, (AP)]. Let assumptions (A4)–(A12) hold. Then the following results hold:*

1. For $p \in C([0, t_f]; \mathbb{R}^m)$, $\lim_{N \rightarrow \infty} J_{(\text{AP})_N}(p) = J_{(\text{P})}(p)$;
2. The mapping $J_{(\text{P})} : C([0, t_f]; \mathbb{R}^m) \rightarrow \mathbb{R}^+$ such that $J_{(\text{P})}(p) = \int_0^{t_f} \text{Tr}(\Pi(t)) dt + J_m(\zeta, p)$ is continuous, where ζ is the sensor state steered by p under the dynamics [2, (2)] and $\Pi(\cdot)$ is the covariance operator obtained through [2, (13)] with sensor state ζ .

Proof of Lemma C.1

1. We first prove that for $p \in C([0, t_f]; \mathbb{R}^m)$,

$$\lim_{N \rightarrow \infty} |J_{(\text{AP})_N}(p) - J_{(\text{P})}(p)| = 0. \quad (7)$$

To establish (7), it suffices to show

$$\lim_{N \rightarrow \infty} \left| \int_0^{t_f} \text{Tr}(\Pi_N(t)) - \text{Tr}(\Pi(t)) dt \right| = 0. \quad (8)$$

We have

$$\begin{aligned} & \left| \int_0^{t_f} \text{Tr}(\Pi_N(t)) - \text{Tr}(\Pi(t)) dt \right| \\ &= \left| \int_0^{t_f} \|\Pi_N(t)\|_{\mathcal{J}_1(\mathcal{H})} - \|\Pi(t)\|_{\mathcal{J}_1(\mathcal{H})} dt \right| \\ &\leq \int_0^{t_f} \left| \|\Pi_N(t)\|_{\mathcal{J}_1(\mathcal{H})} - \|\Pi(t)\|_{\mathcal{J}_1(\mathcal{H})} \right| dt \\ &\leq \int_0^{t_f} \|\Pi_N(t) - \Pi(t)\|_{\mathcal{J}_1(\mathcal{H})} dt \\ &\leq \sup_{t \in [0, t_f]} \|\Pi_N(t) - \Pi(t)\|_{\mathcal{J}_1(\mathcal{H})} t_f. \end{aligned} \quad (9)$$

By [2, Theorem 2.6], $\sup_{t \in [0, t_f]} \|\Pi_N(t) - \Pi(t)\|_{\mathcal{J}_q(\mathcal{H})} \rightarrow 0$ as $N \rightarrow \infty$. And specifically, when $q = 1$, the convergence in (7) holds due to (9).

2. The cost function of (P) is the sum of two parts: the uncertainty cost $\int_0^{t_f} \text{Tr}(\Pi(t)) dt$, cast as a continuous mapping $K : C([0, t_f]; \mathbb{R}^n) \rightarrow \mathbb{R}^+$ (see Lemma 2.5) and the mobility cost $J_m(\zeta, p)$, cast as a mapping $\bar{J}_m : C([0, t_f]; \mathbb{R}^m) \rightarrow \mathbb{R}^+$ which we define below. The mapping \bar{J}_m is the single argument version of the original mobility cost by defining the sensor state as a mapping of the sensor guidance. Here, we redefine the domain of the map T in the proof of [2, Theorem 3.1] such that $T : C([0, t_f]; \mathbb{R}^m) \rightarrow C([0, t_f]; \mathbb{R}^n)$. The continuity of T still holds [4], i.e., for $p_1, p_2 \in C([0, t_f]; \mathbb{R}^m)$ there exist $c_5 > 0$ such that

$$\|Tp_1 - Tp_2\|_{C([0, t_f]; \mathbb{R}^n)} \leq c_5 \|p_1 - p_2\|_{C([0, t_f]; \mathbb{R}^m)}. \quad (10)$$

Let $\bar{J}_m(p) := J_m(Tp, p)$ and we show \bar{J}_m is continuous. Define mappings $G : C([0, t_f]; \mathbb{R}^m) \rightarrow \mathbb{R}^+$, $H : C([0, t_f]; \mathbb{R}^n) \rightarrow \mathbb{R}^+$, and $H_f : C([0, t_f]; \mathbb{R}^n) \rightarrow \mathbb{R}^+$ such that

$$G(p) = \int_0^{t_f} g(p(t), t) dt, \quad (11)$$

$$H(p) = \int_0^{t_f} h(Tp(t), t) dt, \quad (12)$$

$$H_f(p) = h_f(Tp(t_f)). \quad (13)$$

Since $\bar{J}_m(p) = G(p) + H(p) + H_f(p)$, we shall proceed with showing that the mappings G , H , and H_f are continuous.

Let $p_1, p_2 \in \mathcal{P}(p_{\max}, a_{\max})$. Both the set of admissible guidance’s values $P_0 := \cup_{t \in [0, t_f]} \{p(t) : p \in \mathcal{P}(p_{\max}, a_{\max})\}$ and the interval $[0, t_f]$ are closed and bounded (hence compact). Since $g : P_0 \times [0, t_f] \rightarrow \mathbb{R}^+$ is continuous, by the Heine-Cantor Theorem [3, Propo-

sition 5.8.2], g is uniformly continuous, i.e., for all $\epsilon > 0$ there exists $\delta > 0$ such that for all $t \in [0, t_f]$, $|p_1(t) - p_2(t)| < \delta$ implies $|g(p_1(t), t) - g(p_2(t), t)| < \epsilon$. Hence, it follows that

$$\begin{aligned} \|p_1 - p_2\|_{C([0, t_f]; \mathbb{R}^m)} &= \sup_{t \in [0, t_f]} |p_1(t) - p_2(t)| < \delta, \\ \Rightarrow |g(p_1(t), t) - g(p_2(t), t)| &< \epsilon, \quad \forall t \in [0, t_f]. \end{aligned} \quad (14)$$

Therefore, for all $\epsilon > 0$ there exists $\delta > 0$ such that $\|p_1 - p_2\|_{C([0, t_f]; \mathbb{R}^m)} < \delta$ implies

$$\int_0^{t_f} |g(p_1(t), t) - g(p_2(t), t)| dt < \epsilon t_f, \quad (15)$$

which establishes the continuity of the mapping G .

Since the continuous image of a compact set is compact [3, Proposition 5.5.1], the image set $T(\mathcal{P}(p_{\max}, a_{\max}))$ is compact, i.e., the set $\Xi := \{\zeta \in C([0, t_f]; \mathbb{R}^n) : \zeta = Tp, p \in \mathcal{P}(p_{\max}, a_{\max})\}$ is compact. The compactness of Ξ implies that the set of sensor state's values $\zeta(t)$, $\Xi_0 := \cup_{t \in [0, t_f]} \{\zeta(t) | \zeta \in \Xi\}$, is closed. Furthermore, since $\|Tp\|_{C([0, t_f]; \mathbb{R}^n)}$ is bounded (see (10)) and Ξ_0 is finite dimensional, the set Ξ_0 is compact. The compactness of Ξ_0 and continuity of the function $h : \Xi_0 \times [0, t_f] \rightarrow \mathbb{R}^+$ implies that h is uniformly continuous by the Heine-Cantor Theorem [3, Proposition 5.8.2]. Hence, for all $\epsilon > 0$ there exists $\delta > 0$ such that if $\|p_1 - p_2\|_{C([0, t_f]; \mathbb{R}^m)} < \delta/c_5$, which implies $\|Tp_1 - Tp_2\|_{C([0, t_f]; \mathbb{R}^n)} < \delta$, then

$$\int_0^{t_f} |h(Tp_1(t), t) - h(Tp_2(t), t)| dt \leq \epsilon t_f, \quad (16)$$

which concludes the continuity of the mapping H .

The mapping H_f is continuous because for all $\epsilon > 0$ there exists $\delta > 0$ such that if $\|p_1 - p_2\|_{C([0, t_f]; \mathbb{R}^m)} < \delta/c_5$, which implies $\sup_{t \in [0, t_f]} |Tp_1(t) - Tp_2(t)| < \delta$, then

$$|Tp_1(t_f) - Tp_2(t_f)| < \delta. \quad (17)$$

Furthermore, $|H_f(p_1) - H_f(p_2)| = |h_f(Tp_1(t_f)) - h_f(Tp_2(t_f))| < \epsilon$ holds due to the continuity of h_f .

Hence, we conclude the continuity of \bar{J}_m , which, together with the continuity of $K(\cdot)$ and (10), implies the continuity of $J_{(P)}(\cdot)$. \square

References

- [1] J. A. Burns and C. N. Rautenberg. The infinite-dimensional optimal filtering problem with mobile and stationary sensor networks. *Numer. Funct. Anal. Optim.*, 36(2):181–224, 2015.
- [2] S. Cheng and D. A. Paley. Optimal guidance and estimation of a 2D diffusion-advection process by a team of mobile sensors. *Accepted for publication in Automatica*, 2021.
- [3] W. A. Sutherland. *Introduction to metric and topological spaces*. Oxford University Press, 2009.
- [4] J. Werner. *Optimization theory and applications*. Springer-Verlag, 2013.